Scientific Reports

https://doi.org/10.1038/s41598-026-35686-0

Article in Press

Rational redesign of high-activity G-quadruplex DNAzyme through flanking and looping of nucleobases

Received: 7 October 2025

Accepted: 7 January 2026

Published online: 12 January 2026

Cite this article as: Adeoye R.I., Babbudas N., Birchenough M. *et al.* Rational redesign of high-activity G-quadruplex DNAzyme through flanking and looping of nucleobases. *Sci Rep* (2026). https://doi.org/10.1038/s41598-026-35686-0

Raphael I. Adeoye, Nikhildas Babbudas, Matthew Birchenough, Francesca Giuntini & Femi J. Olorunniji

Rational Redesign of High-Activity G-quadruplex DNAzyme Through Flanking and Looping of Nucleobases

Raphael I. Adeoye, Nikhildas Babbudas, Matthew Birchenough, Francesca Giuntini and Femi J. Olorunniji*

School of Pharmacy & Biomolecular Sciences, Faculty of Health, Innovation, Technology and Science, Liverpool John Moores University, Liverpool L3 3AF, UK

* Corresponding Author: Femi J. Olorunniji

Email: F.J.Olorunniji@ljmu.ac.uk; ORCID: 0000-0001-9389-2981

Abstract

G-quadruplex (G4) DNAzymes are guanine-rich oligonucleotides with intrinsic peroxidase-mimicking activity upon complexation with hemin, offering a promising alternative to protein-based enzymes in biosensing. However, their relatively low catalytic efficiency limits practical applications. Here, we present a structure-guided redesign of the high-activity aptamer [B7]-3-0 by incorporating strategic flanking and looping nucleobase modifications. Introduction of adenine and thymine–cytosine elements at the 3′ end led to up to 4-fold enhancements in reaction extent and a 3-fold increase in initial velocity under moderate hydrogen peroxide conditions (0.425 mM). Remarkably, the modified B730 variants retained activity at elevated H_2O_2 concentrations (4.25 mM), achieving up to 8-fold catalytic enhancement and outperforming high-activity DNAzymes including AS1411 and CatG4. These redesigned DNAzymes demonstrated improved peroxidase activity and resistance to oxidative inactivation, addressing a major limitation of both natural and artificial peroxidases. Our findings establish flanking and loop engineering as a cost-effective and broadly applicable strategy for optimizing G4 DNAzymes and underscore their potential in the development of next-generation biosensors.

Keywords: G-quadruplex, DNAzymes, peroxidase, rate-enhancement.

Introduction

Aptamers are single-stranded oligonucleotides selected through *in vitro* screening for their ability to bind specific molecules, ions, or proteins with high affinity. They often exhibit greater specificity than typical antibody-antigen interactions. Aptamers can adopt various secondary structures such as loops, bulges, stems, pseudoknots, and G-quadruplexes [1]. G-quadruplexes (G4s) are formed by the stacking of G-quartets, planar assemblies of guanine bases connected via Hoogsteen hydrogen bonding. These structures arise from guanine-rich sequences in the presence of potassium ions, which coordinate with the oxygen atoms of guanine bases. When complexed with hemin (a cofactor in many oxidase systems), G4 structures function as DNAzymes with peroxidase-mimicking activity, using the same mechanism as the protein peroxidases (Figure 1). These G4 DNAzymes are thermally and chemically stable, compact, inexpensive to produce, and easy to modify. Their molecular recognition abilities, programmability, and adaptability make them highly attractive for applications in biosensing and biotechnology [2]. Hemin's planar aromatic structure allows π-π stacking interactions with the aromatic rings of bases in the external 3′-terminal G4. The accessibility of terminal G-quartets significantly influences hemin binding and, consequently, the catalytic efficiency of the G4 DNAzyme.

By modifying oligonucleotide sequences and incorporating specific recognition elements, G4 DNAzyme-based biosensors can be engineered to detect a wide range of analytes with high precision. The ability of G-quadruplex structures to form functional nucleic acids through aptamer recognition sites has significantly heightened interest in their application for biomolecular sensing [3]. These DNA-based catalysts offer exceptional versatility in diagnostic platforms, effectively detecting nucleic acids, proteins, and other biologically relevant molecules associated with pathogenic organisms. Their adaptability spans multiple detection modalities including chemiluminescent, colorimetric, and electrochemical techniques. Furthermore, their performance can be enhanced by integration with advanced technologies such as isothermal PCR, DNA walkers, and the CRISPR-Cas system, which boosts both specificity and sensitivity [4].

Despite these advantages, G4 DNAzymes typically exhibit lower catalytic activity compared to natural peroxidases. Traditional nucleic acid detection methods often rely heavily on target amplification (e.g., PCR) or labelling, which increases complexity, cost, and the risk of contamination. To address these limitations, researchers have explored strategies to enhance DNAzyme catalytic efficiency. One such approach involves the addition of exogenous reagents, such as ATP and spermine, that modestly improve reaction rates [5–7]. However, these additives must be used at high concentrations, contributing to elevated costs while still falling short of the catalytic performance seen in natural enzymes. Despite ongoing progress, a degree of ambiguity remains regarding how specific modifications influence the catalytic activity of G4 DNAzymes, as their response

to activation varies by sequence type. Previous studies have proposed that multimerisation can enhance catalytic efficiency by providing multiple active sites for hemin binding [2,8–10]. However, not all multimeric G4 DNAzymes yield synergistic or cooperative rate enhancement. In some cases, steric hindrance from bulky groups impedes effective π–π stacking, limiting hemin binding to the G-quartet and ultimately reducing catalytic efficiency, even in parallel structures.

Several approaches have been adopted to address these challenges. For instance, Kosman *et al.* [11] showed enhanced activity through covalent G4-hemin linkage. Cheng *et al*. [9] demonstrated that covalent dimerization of G4/hemin constructs significantly boosted biocatalytic performance by providing a preconfigured active site for H_2O_2-driven activation. Similarly, Li *et al*. [12] introduced a “zippered” G4/hemin DNAzyme formed by hybridising short oligonucleotides near complementary G4 sequences, facilitating hemin interaction and improving peroxidase-mimicking activity. Beyond traditional 5′-3′ phosphodiester linkages, inversion of polarity sites (3′-3′ or 5′-5′ linkages) also offer structural advantages. [13] reported enhanced peroxidase activity in G4 DNAzymes featuring dual 3′-terminal G-tetrads in inverted configurations.

Conventionally, catalytically active G4 DNAzymes are isolated via SELEX, primarily based on hemin-binding affinity. However, post-SELEX modifications have emerged as a promising route to elevate activity, independent of binding affinity. Alterations in the catalytic core, such as base substitutions or extensions, can significantly impact performance. Notably, interactions between hemin and the bases in G4 loops and flanks have been shown to modulate redox activity. Incorporating specific nitrogenous bases within flanks, bulges, or linkers has become a targeted strategy for catalytic enhancement. Chang *et al*. [14] found that flanking the G4 sequence with d(CCC) increased DNAzyme activity and broadened its pH tolerance. Similarly, Guo *et al*. [15] demonstrated improved catalytic efficiency when adenine bases were flanked at both ends of the G-tract. While these loop and linker regions do not directly participate in G-quartet formation, structural studies (e.g., CD and NMR) reveal that such modifications do not disrupt parallel G4 conformations but still modulate activity. The precise molecular mechanisms behind this enhancement remain unclear, as changes in conformation, thermal stability, or hemin-binding affinity have not fully explained the observed improvements. Nonetheless, the overall catalytic activity of modified G4 DNAzymes, such as those flanked by adenine, still lags natural peroxidases.

Zhu *et al.* [16] identified a highly active 20-nucleotide truncated aptamer, [B7]-3-0, here abbreviated as B730, selected via hemin-SELEX from an 81-nt ssDNA library with varying guanine content. B730 exists in a parallel configuration and it outperformed earlier designs like PS2.M and EAD2, representing a significant improvement in the catalytic performance of G-quadruplex DNAzymes. B730 remains one of the most active G4 DNAzymes without additional covalent modification and is often used to benchmark the peroxidase activities of novel aptamers [17].

In this work, our aim is to better understand how the type and positional arrangement of nucleobases in flanks, linkers, and loops influence the catalytic activity of DNAzymes. We used B730 as a model system to show how a systematic approach can guide the rational design of next-generation high-activity G4 DNAzymes, using steps that do not require lengthy iterative process of directed evolution. We designed a variant of B730 with high activity and significant resistance to inactivation to high H_2O_2 concentration, demonstrating that the strategy provides a simple, cost-effective framework for designing highly active and inactivation-resistant G4 DNAzymes with improved functional resilience.

Materials and Methods

Reagents

High-performance liquid chromatography (HPLC)-purified DNA oligonucleotides were obtained from Integrated DNA Technologies (Leuven, Belgium). Stock solutions (100 µM) were prepared by resuspending the oligonucleotides in Tris-EDTA buffer (10 mM Tris-HCl, pH 7.5; 0.1 mM EDTA) in volumes specified in the synthesis report and stored at −20 °C in Nunc tubes until use. Oligonucleotide concentrations were confirmed via absorbance at 260 nm (A_{260}) measurements, with sequence-specific molecular weights applied for calculations.

The following reagents were used: 2,2′-azinobis(3-ethylbenzthiazoline)-6-sulfonic acid (ABTS), hemin, ethylenediaminetetraacetic acid (EDTA), tris(hydroxymethyl) amino- methane (Tris), 2-[N-morpholino] ethanesulfonic acid (MES), dimethyl sulfoxide (DMSO), hydrogen peroxide (H_2O_2), and Triton X-100 (all from Sigma-Aldrich, Dorset, UK). Potassium chloride (KCl) and sodium chloride (NaCl) were purchased from Fisher Scientific (Leicestershire, UK).

Preparation of DNAzyme (Oligonucleotide-Hemin complex)

DNAzymes were prepared by complexing oligonucleotides with hemin to yield a 10 µM catalytically active unit, as previously described [7]µL of 100 µM oligonucleotide solution was added to 450 µL of reaction buffer RB1 (25 mM MES, pH 5.5; 20 mM KCl; 200 mM NaCl; 0.05% Triton X-100; 1% DMSO), heated to 95 °C for 10 minutes, rapidly cooled on ice for 15 minutes (0 °C), and equilibrated at 25 °C for another 15 minutes to facilitate G-quadruplex formation. To assemble the catalytic complex, 10 µL of 100 µM of hemin solution was added, mixed thoroughly, and incubated at 25 °C for 30 minutes.

Determination of peroxidase activity of DNAzymes

Peroxidase activity of the DNAzyme (0.25 µM) was assessed in RB1 containing 2.5 mM ABTS and 0.425 mM H_2O_2. The reaction was initiated by addition of H_2O_2, and absorbance was monitored immediately at 415 nm every 5 seconds for 3 minutes using a CLARIOstar Plate Reader (BMG LABTECH). Initial velocities (Vo) were determined from the linear portion of the absorbance-time curve and calculated by dividing the rate of absorbance change by the extinction coefficient of ABTS, as previously established [2,7].

Inactivation kinetics

The effect of increasing H_2O_2 concentrations on DNAzyme inactivation was evaluated for both wild-type and modified constructs. Reactions contained 0.25 µM DNAzyme, 2.5 mM ABTS, and H_2O_2 concentrations ranging from 0.106 to 4.250 mM (0.106, 0.213, 0.319, 0.425, 1.063, 2.125, 3.188, 4.250 mM). Absorbance changes were recorded as previously described [2,18].

Circular dichroism spectra

Circular dichroism (CD) spectra (320–220 nm) were recorded for 10 µM G4 oligonucleotides in 25 mM MES buffer (pH 5.5) containing K^+ ions with Jasco J-1100 CD spectrometer (Japan), to evaluate G-quadruplex conformation [14,19–24]A 4 mm path cell, 1 nm bandwidth, 0.1 data pitch and a scanning speed of 200 nm/min was used to collect average of three scans at 22 ^oC with MES buffer as baseline control.

Relative amount of compound I formed

Formation of Compound I, a transient peroxidase intermediate, was analysed by monitoring absorbance at 404 nm over time following the addition of 1 mM H_2O_2 to 1 µM DNAzyme. The degradation rate, reflective of Compound I formation, was calculated from the initial slope of the absorbance-time curve for both wild-type and modified DNAzyme variants [14,21,23].

Results

Preliminary modifications to the B730 aptamer sequence

We performed a structure-guided redesign of the truncated high-activity G4 DNAzyme B730 by introducing flanking and looping nucleobases (Table 1). Adenine residues were inserted at various loop positions within the G-tracts, and their number at the 3′ end was varied. All reactions were conducted in MES buffer (pH 5.5), chosen for its ability to stabilize the reducing substrate ABTS and its alignment with the pKa of nucleobases, thereby favouring ionization of reactive groups. Since the pKa of hemin is approximately 4.36 [25], this shared chemical environment may enhance peroxidase activity by accelerating Compound I formation [20].

Since some studies specifically on the effect of 3’ terminal adenine and cytosine nucleobases on the activities of G4 DNAzymes have been carried out in MES buffer ranging from pH 5.1 to 5.5 [15,19, 26] rather than at pH 7.0 reported for most studies, we carried out an initial comparison of activities at pH 5.5 and pH 7.0. We tested the activities of B730 and B730-1 in reaction buffers with MES pH 5.5 and HEPES pH 7. Although, there was no difference in the reaction extent from the two DNAzymes at pH 7.0, the DNAzyme with the 3’ modification was more active in MES pH5.5; maintaining a linear increase up till 180 seconds while the reaction of the unmodified base peaked after 50 seconds (data not shown).

The catalytic activities of each variant were assessed by monitoring ABTS oxidation kinetics in the presence of H_2O_2 (Figure 2). Initial velocities for B730, B730-1, B730-2, B730-3, B730-4, and B730-5 were 51, 116, 100, 110, 110, and

110 nM/s, respectively. Corresponding reaction extents after 3 minutes were 3.49, 10.4, 8.69, 9.53, 9.38, and 9.23 µM. These results indicate that adenine looping within the G-tracts and flanking adenines at the 3′ end consistently enhanced both initial reaction rates (~2-fold) and total product accumulation (~3-fold) relative to unmodified B730.

Rate enhancement by flanking adenine and thymine-cytosine (TC)

Previous studies have shown that 3′-end flanking regions in G4 DNAzymes not only contribute to hemin binding but also facilitate substrate positioning via axial coordination, enhancing the rate of Compound I formation, the rate-limiting step in the peroxidase cycle [14,19–24]. To fine-tune the spatial arrangement between the G4 catalytic core and hemin's hexacoordinated iron centre, we replaced the 3′ terminal adenine in B730-1 (the most active of the 5 variants) with a Thymine-Cytosine (TC) dinucleotide to create B730-1.2 (Table 1). This modification was inspired by earlier findings that TC addition at the 3′ end of the G3T sequence enhances peroxidase activity [22,24]. As anticipated, the combination of looped adenines and a TC tail in B730-1.2 resulted in a 3-fold increase in initial velocity and a 4-fold increase in reaction extent compared to the parent B730 sequence (Figure 3).

Comparison of activity of B730-1.2 with other high activity DNAzymes

To assess the performance of B730-1.2, we compared its catalytic efficiency with two well-characterized high-activity DNAzymes: AS1411 and CatG4 [2,5,27]nucleolin-binding aptamer with anticancer properties and has been extensively evaluated for peroxidase activity. Remarkably, B730-1.2 outperformed both AS1411 and CatG4, exhibiting higher initial velocity and product yield. The initial velocities (V_0) of B730-1.2, AS1411 and CatG4 at 0.25 µM DNAzyme, 2.5 mM ABTS and 0.425 mM H_2O_2 are 154, 53 and 100 nM/s respectively; while the extent of ABTS oxidation after 3 minutes are 13.6, 4.76 and 10.5 µM respectively in MES buffer pH 5.5 (Figure 3).

We investigated the activities of the three DNAzymes at different DNAzyme concentrations [E] to determine the relative turnover rates. The specific activities (V_0/[E]) determined for B730-1.2, AS1411 and CatG4 were 574.2, 197.2 and 395.4 mM/s, respectively (Figure 4), showing that B730-1.2 is a significant improvement on non-modified DNA aptamers currently in use as G4 DNAzymes.

B730-1.2 displays stable activity in the presence of high H_2O_2 concentration.

Both natural peroxidases and G4 DNAzymes are prone to oxidative inactivation at high H_2O_2 concentrations due to accumulation of Compound III (peroxyiron(III) porphyrin radical), which irreversibly degrades the hemin cofactor [28–30]stability under this inactivating condition, we evaluated the activities of B730-1.2, CatG4, and AS1411 under increasing H_2O_2 concentrations at low (0.01 µM) and optimal (0.25 µM) DNAzyme concentrations (Figures 5 and 6).

B730-1.2 exhibited substantial tolerance to high H_2O_2 concentration, maintaining activity even at 4.25 mM H_2O_2. Under these conditions, its initial velocity increased by 5- to 8-fold relative to the wild-type B730, and significantly more active than CatG4 and AS1411. To further test the resilience of the DNAzymes to

inactivation induced by exposure to very high H_2O_2 concentrations, we tested their activities using very low DNAzyme concentration (0.05 µM). Under these conditions, the very high H_2O_2/DNAzyme ratio would normally trigger irreversible inactivation and decrease in peroxidase activity for G4 DNAzymes and natural peroxidases [2,29] As shown in Figure 7, B730-1.2, CatG4 and AS1411 displayed initial velocities of 2310, 370 and 1200 nM/s at 50 mM H_2O_2, indicating that the modified B730 variant was more resilient to inactivating conditions than the two controls we used. The higher activities suggest that in the absence of inactivating events, the rate of reaction catalysed by G4 DNAzymes can be enhanced by using higher H_2O_2 concentrations.

Circular dichroism spectra reveal preserved G4 folding

To confirm whether the sequence modifications we made to B730 altered their G4 structures, we determined circular dichroism spectra of the G4 sequences, the standard approach used in similar studies that investigated the mechanism of terminal nucleobase addition on rate enhancement [11,15,19,21]. We collected circular dichroism spectra (220–320 nm) for wild-type and variant sequences (Figure 8). Both B730-1 and B730-1.2 exhibited characteristic peaks of parallel G4 topology: positive peak at ~265 nm and negative peak at ~240 nm [16,20,23] strategy with native folding.

Enhanced compound I formation in B730 and its variant

To explore the mechanistic basis for the observed catalytic enhancement, we monitored the formation of Compound I, the oxoiron(IV) porphyrin radical cation intermediate that mediates the initial oxidation step of the peroxidation reaction, by tracking absorbance at 404 nm following H_2O_2 addition [14,21,23]DNAzymes, formation of Compound I is the key rate-limiting transition from ferric hemin to the reactive catalytic state. Variants of B730 demonstrated more rapid Compound I formation than the wild type, confirming that peripheral base modifications accelerate activation of the DNAzyme–hemin complex (Figure 9).

Discussion

In this study, we show that modifying flanking and loop-region nucleobases enhances the intrinsic peroxidase activity of G4 DNAzymes. Our best construct, B730-1.2, showed 3-fold enhancement of activity compared to the unmodified B730 aptamer, which is one of the best non-modified G4 DNAzymes reported so far [16]. Bhuyan et al. [17] used directed evolution to design a novel G4 DNAzyme, msBDZ-X-3, that was at best twice as active as B730 in all assay conditions. Although, we have not made a direct comparison between B730-1.2 and msBDZ-X-3 in this work, the comparisons with B730 here and in that study suggest that B730-1.2 could be the most active non-modified G4-quadruplex DNAzymes reported to date. Although higher activities have been reported when G4 DNAzymes are covalent modified by chemical linkage with hemin or other cofactors [17,31], the additional cost and complexities associated with making

these covalent modifications limit their incorporation into routine diagnostic or biosensing applications.

The data presented in this study are not sufficient to provide direct explanations for the mechanistic basis for the enhanced activities and stability of B730-1.2, but the modifications made are similar in design to those reported earlier in the literature suggesting that the changes likely creates a localized, buffered microenvironment that sustains catalysis even at elevated H_2O_2 concentrations. Studies in which the rate enhancement effects of the adenine and TC nucleobases were investigated showed that the terminal 3' base modifications did not affect the binding of hemin to the DNA sequences of both the parent sequence and the modified one [15,19,21]. G-quadruplex (G4) DNAzymes derive their catalytic power from a finely tuned interplay of structural elements: a hydrophobic hemin binding pocket, monovalent cation (e.g., K^+) coordination sites that stabilize the G4 fold, substrate recognition regions, and residues that stabilize reaction intermediates and facilitate proton transfer [20]. Enhanced folding stability and optimized stacking interactions between guanine quartets and hemin have been linked to improved catalytic activity [16].

One likely explanation for the observed increased activity of the modified sequences at pH 5.5 may be due to increased tendency to deprotonate adenine and cytosine and make them facilitate redox reaction by acting as general acid-base species in G4 DNAzyme reactions in a way similar to the role of distal histidine in natural peroxidase reactions. The pKa of adenine and cytosine are 4.2 and 4.6, respectively, which is closer to pH 5.5 than pH 7 that seems to work better for G4 sequences with no terminal adenine or guanine bases. Similar effects were observed in earlier studies in which flanking nucleobases were studied. Guo et al. [15] (SI Fig 10) reported high activity for DNAzyme flanked with nucleobases at pH 5.5 than pH 7. Li et al. [19] also reported high activity at pH 5.1 in various nitrogenous and oxyanion buffers for modified G4 DNAzyme.

Parallels between these synthetic systems and natural peroxidases such as horseradish peroxidase provide mechanistic insights. Key catalytic residues including His170 (proximal ligand), His42, and Arg38 (distal ligands) orchestrate the conversion of ferric-hydroperoxide to the highly reactive Fe(IV)=O (Compound I) species [32]. In G4 DNAzymes, loop and flanking regions can functionally mimic these residues, influencing substrate access, folding topology, and catalytic turnover. Several studies have established that the mechanism through which the adenine residues at the 3' end enhance activity is to mimic the histidine residue at the active centre of natural peroxidases [15,19,21,26]. In this role, a cascade of redox reactions leads to the increase in the formation of Compound I, the rate-limiting catalytic entity in peroxidase reactions. Our result of the initial degradation velocity of DNAzymes when exposed to H_2O_2 provided mechanistic insight that the enhanced catalytic activity of the modified DNAzyme was due to rate of compound I formation.

Our circular dichroism spectral data suggest parallel G4 conformation for B730 based on positive peak at 264 nm and negative peak at 240 nm; this agrees with

initial report by Zhu et al. [16]. Similar G4 conformations suggests that flanking and loop modifications enhances peroxidase activity by a different mechanism other than structural alteration. The 2’ methyl modification in B730 has been reported to stabilise their parallel conformation, thermal stability and by extension their peroxidase activity [16]. Potassium ions are well known to stabilize this parallel topology, and their presence likely maintained conformational integrity across variants, even following hemin complexation [33]. Minor increases in thermal stability as shown through melting temperatures of 68.7, 69.5, and 70.1 °C for B730, B730-1, and B730-1.2, respectively suggest that rate enhancement stems not from global stabilization, but from fine-tuned molecular interactions at the catalytic interface. Our findings based on CD spectral analyses agree with earlier studies that the 3’ nucleobase additions did not change the overall G4 topology of the modified sequences [15,19,21,26].

Adenine residues, especially in 3′ flanking positions, may accelerate Compound I formation by mimicking the distal histidine’s role in general acid-base catalysis [19]. The unprotonated N1 of adenine can directly interact with H_2O_2, facilitating O-O bond cleavage, a key step in peroxidase catalysis. Furthermore, flanking bases may support proper alignment of hemin with the G4 scaffold, improving electron transfer, folding kinetics, and hemin accessibility [19,20]. Enhanced π–π stacking and electrostatic interactions from additional adenines may also contribute to hemin stabilization [19].

Our B730-1.2 variant, incorporating a 3′-terminal TC dinucleotide, further optimized the catalytic interface. Molecular modelling studies carried out by Li et al. [19] and Qiu et al. [22] suggest that the hemin centre sits ~4.5–5.9 Å from the N3 and 4-NH_2 atoms of dC in TC-flanked G4s, distances suitable for forming dual hydrogen bonds with H_2O_2. Although thymine lacks amino or basic nitrogen atoms, its compact pyrimidine structure likely helps position cytosine favourably relative to the iron centre. In contrast, bulkier purine rings in adenine may impose less optimal spatial constraints. Thus, the TC flanks appear to balance proximity, orientation, and chemical functionality, enhancing substrate coordination and catalytic efficiency [24].

Resistance to inactivation under high H_2O_2 concentration conditions is a major advantage of the redesigned B730-derived DNAzyme. In conventional peroxidases, Compound I (Fe(IV)=O $^+$ radical) is formed by heterolytic cleavage of H_2O_2 and normally proceeds via two one-electron reductions to regenerate the resting ferric state [34]. Under excess H_2O_2, however, these enzymes often form Compound III, an inactive peroxyiron(III) species that triggers haem degradation [29,30]. This vulnerability is exacerbated by the Fe^{3+} redox centre’s susceptibility to radical attack [35]. Remarkably, our flanking and looping modifications appear to mitigate this inactivation pathway. We hypothesize that adenine and Thymine-Cytosine bases help shuttle electrons and stabilise catalytic intermediates, shielding the hemin cofactor from oxidative damage.

Conclusion

This study demonstrates that rationally designed flanking and loop modifications can significantly enhance the peroxidase activity and oxidative resilience of G4

DNAzymes. Strategic incorporation of adenine and TC motifs at the 3′ end of the B730 aptamer created a microenvironment conducive to faster Compound I formation, the rate-limiting step in the catalytic cycle. These structural adjustments improved catalytic turnover and enabled the DNAzyme to function under elevated H_2O_2 concentrations, where conventional DNAzymes often fail.

Our findings establish flanking and loop engineering as a simple, cost-effective, and scalable strategy for developing robust G4 DNAzymes for biosensing applications. Importantly, the modifications preserve the inherent simplicity and parallel topology of the G4 scaffold while unlocking higher activity and chemical durability. This approach lays the groundwork for next-generation DNAzyme designs in diagnostics, environmental monitoring, and synthetic biocatalysis.

Author Contributions: Conceptualisation: Raphael I. Adeoye and Femi J. Olorunniji; Methodology: Raphael I. Adeoye, Francesca Giuntini and Femi J. Olorunniji; Investigation: Raphael I. Adeoye, Nikhil Babbudas and Matthew Birchenough; Writing—Original Draft: Raphael I. Adeoye, Nikhil Babbudas, Matty Birchenough, and Femi J. Olorunniji; Writing—Review and Editing: Raphael I. Adeoye, Francesca Giuntini and Femi J. Olorunniji; Formal Analysis, Visualisation and Data Curation: Raphael I. Adeoye and Femi J. Olorunniji; Supervision and Project Administration, Femi J. Olorunniji; Funding Acquisition: Raphael I. Adeoye and Femi J. Olorunniji. All authors have read and agreed to the published version of the manuscript.

Funding: This research was supported by institutional funding from Liverpool John Moores University, Liverpool, U.K.

Institutional Review Board Statement: Not applicable.

Data Availability Statement: All data generated or analysed during this study are included in this published article.

Declarations

Ethics Approval Not applicable.

Consent to Participate Not applicable

Consent for Publication Not applicable

Competing Interests: None.

References

1. Liu, R., Li, J., Salena, B. J. & Li, Y. (2025). Aptamer and DNAzyme Based Colorimetric Biosensors for Pathogen Detection. *Angewandte Chemie International Edition*, *64*(4), e202418725.
2. Adeoye, R. I., Osalaye, D. S., Ralebitso-Senior, T. K., Boddis, A., Reid, A. J., Fatokun, A. A., Powell, A. K., Malomo, S. O. & Olorunniji, F. J. (2019).

Catalytic activities of multimeric G-quadruplex DNAzymes. *Catalysts*, *9*(7), 613.

3. Sahayasheela, V. J. & Sugiyama, H. (2024). RNA G-quadruplex in functional regulation of noncoding RNA: Challenges and emerging opportunities. *Cell Chemical Biology*, *31*(1), 53–70.
4. Wang, Y., Xiao, J., Lin, X., Waheed, A., Ravikumar, A., Zhang, Z., Zou, Y. & Chen, C. (2023). A self-assembled G-quadruplex/hemin DNAzyme-driven DNA walker strategy for sensitive and rapid detection of lead ions based on rolling circle amplification. *Biosensors*, *13*(8), 761.
5. Kong, D. M., Xu, J. & Shen, H. X. (2010). Positive effects of ATP on G-quadruplex-hemin DNAzyme-mediated reactions. *Analytical Chemistry*, *82*(14), 6148–6153.
6. Qi, C., Zhang, N., Yan, J., Liu, X., Bing, T., Mei, H. & Shangguan, D. (2014). Activity enhancement of G-quadruplex/hemin DNAzyme by spermine. *RSC Advances*, *4*(3), 1441–1448.
7. Adeoye, R. I., Ralebitso-Senior, T. K., Boddis, A., Reid, A. J., Giuntini, F., Fatokun, A. A., Powell, A. K., Ihekwaba-Ndibe, A., Malomo, S. O. & Olorunniji, F. J. (2025). Spermine Enhances the Peroxidase Activities of Multimeric Antiparallel G-quadruplex DNAzymes. *Biosensors*, *15*(1), 12.
8. Stefan, L., Denat, F. & Monchaud, D. (2011). Deciphering the DNAzyme activity of multimeric quadruplexes: insights into their actual role in the telomerase activity evaluation assay. *Journal of the American Chemical Society*, *133*(50), 20405–20415.
9. Cheng, Y., Cheng, M., Hao, J., Jia, G., Monchaud, D. & Li, C. (2020). The noncovalent dimerization of a G-quadruplex/hemin DNAzyme improves its biocatalytic properties. *Chemical Science*, *11*(33), 8846–8853.
10. Zhang, Y., Ma, X., Zhang, J., Luo, F., Wang, W. & Cui, X. (2021). Design of a high-sensitivity dimeric G-quadruplex/hemin DNAzyme biosensor for norovirus detection. *Molecules*, *26*(23), 7352.
11. Kosman, J., Żukowski, K. & Juskowiak, B. (2018). Comparison of Characteristics and DNAzyme Activity of G4–Hemin Conjugates Obtained via Two Hemin Attachment Methods. *Molecules*, *23*(6), 1400.
12. Li, J., Wu, H., Yan, Y., Yuan, T., Shu, Y., Gao, X., Zhang, L., Li, S., Ding, S. & Cheng, W. (2021). Zippered G-quadruplex/hemin DNAzyme: exceptional catalyst for universal bioanalytical applications. *Nucleic Acids Research*, *49*(22), 13031–13044.
13. Virgilio, A., Esposito, V., Lejault, P., Monchaud, D. & Galeone, A. (2020). Improved performances of catalytic G-quadruplexes (G4-DNAzymes) via the chemical modifications of the DNA backbone to provide G-quadruplexes with double 3′-external G-quartets. *International Journal of Biological Macromolecules*, *151*, 976–983.
14. Chang, T., Gong, H., Ding, P., Liu, X., Li, W., Bing, T., Cao, Z. & Shangguan, D. (2016). Activity Enhancement of G-Quadruplex/Hemin DNAzyme by Flanking d (CCC). *Chemistry–A European Journal*, *22*(12), 4015–4021.

15. Guo, Y., Chen, J., Cheng, M., Monchaud, D., Zhou, J. & Ju, H. (2017). A Thermophilic Tetramolecular G-Quadruplex/Hemin DNAzyme. *Angewandte Chemie International Edition*, *56*(52), 16636–16640.
16. Zhu, L., Li, C., Zhu, Z., Liu, D., Zou, Y., Wang, C., Fu, H. & Yang, C. J. (2012). In vitro selection of highly efficient G-quadruplex-based DNAzymes. *Analytical Chemistry*, *84*(19), 8383–8390.
17. Bhuyan, S. K., Wang, L., Jinata, C., Kinghorn, A. B., Liu, M., He, W., Sharma, R. & Tanner, J. A. (2023). Directed evolution of a G-quadruplex peroxidase DNAzyme and application in proteomic DNAzyme–aptamer proximity labeling. *Journal of the American Chemical Society*, *145*(23), 12726–12736.
18. Yang, X., Fang, C., Mei, H., Chang, T., Cao, Z. & Shangguan, D. (2011). Characterization of G-quadruplex/hemin peroxidase: substrate specificity and inactivation kinetics. *Chemistry–A European Journal*, *17*(51), 14475–14484.
19. Li, W., Li, Y., Liu, Z., Lin, B., Yi, H., Xu, F., Nie, Z. & Yao, S. (2016). Insight into G-quadruplex-hemin DNAzyme/RNAzyme: adjacent adenine as the intramolecular species for remarkable enhancement of enzymatic activity. *Nucleic Acids Research*, *44*(15), 7373–7384.
20. Chen, J., Guo, Y., Zhou, J. & Ju, H. (2017). The Effect of Adenine Repeats on G-quadruplex/hemin Peroxidase Mimicking DNAzyme Activity. *Chemistry–A European Journal*, *23*(17), 4210–4215.
21. Chen, J., Zhang, Y., Cheng, M., Guo, Y., Šponer, J., Monchaud, D., Mergny, J.-L., Ju, H. & Zhou, J. (2018). How proximal nucleobases regulate the catalytic activity of G-quadruplex/hemin DNAzymes. *ACS Catalysis*, *8*(12), 11352–11361.
22. Qiu, D., Mo, J., Liu, Y., Zhang, J., Cheng, Y. & Zhang, X. (2020). Effect of distance from catalytic synergy group to iron porphyrin center on activity of G-quadruplex/hemin DNAzyme. *Molecules*, *25*(15), 3425.
23. Cao, Y., Ding, P., Yang, L., Li, W., Luo, Y., Wang, J. & Pei, R. (2020). Investigation and improvement of catalytic activity of G-quadruplex/hemin DNAzymes using designed terminal G-tetrads with deoxyadenosine caps. *Chemical Science*, *11*(26), 6896–6906.
24. Connelly, R. P., Fonseca, V. & Gerasimova, Y. V. (2025). Peroxidase-like Activity of G-Quadruplex/Hemin Complexes for Colorimetric Nucleic Acid Analysis: Loop and Flanking Sequences Affect Signal Intensity. *DNA*, *5*(1), 12.
25. Kong, D.-M., Wu, J., Wang, N., Yang, W. & Shen, H.-X. (2009). Peroxidase activity–structure relationship of the intermolecular four-stranded G-quadruplex–hemin complexes and their application in Hg2+ ion detection. *Talanta*, *80*(2), 459–465.
26. Udomprasert, A., Chimasungkanun, S. and Kangsamaksin, T. (2025). Kinetic analysis of catalytic activity of G-quadruplex/hemin DNAzyme with flanking adenine nucleotides. *Scientific Reports*, *15*(1), p.40260.
27. Bagheri, Z., Ranjbar, B., Latifi, H., Zibaii, M. I., Moghadam, T. T. & Azizi, A. (2015). Spectral properties and thermal stability of AS1411 G-

quadruplex. *International Journal of Biological Macromolecules*, *72*, 806–811.
28. Vazquez-Duhalt, R. (1999). Cytochrome c as a biocatalyst. *Journal of Molecular Catalysis B: Enzymatic*, *7*(1–4), 241–249.
29. Valderrama, B., Ayala, M. & Vazquez-Duhalt, R. (2002). Suicide inactivation of peroxidases and the challenge of engineering more robust enzymes. *Chemistry & Biology*, *9*(5), 555–565.
30. Monte Carlo III, A. R. & Fu, J. (2022). Inactivation Kinetics of G-Quadruplex/Hemin Complex and Optimization for More Reliable Catalysis. *ChemPlusChem*, *87*(7), e202200090.
31. Li, J., Jiang, L., Wu, H., Zou, Y., Zhu, S., Huang, Y., Hu, X., Bai, H., Li, Y. & Zou, Y. (2025). Self-contained G-quadruplex/hemin DNAzyme: a superior ready-made catalyst for in situ imaging analysis. *Nucleic Acids Research*, *53*(6), gkaf227.
32. Liu, B., Wang, T., Qiu, D., Yan, X., Liu, Y., Mergny, J.-L., Zhang, X., Monchaud, D., Ju, H. & Zhou, J. (2024). Arginine-Modified Hemin Enhances G-Quadruplex DNAzyme Peroxidase Activity for High Sensitivity Detection. *Analytical Chemistry*, *96*(36), 14590–14597.
33. Cheng, Y., Cheng, M., Hao, J., Miao, W., Zhou, W., Jia, G. & Li, C. (2021). Highly selective detection of K+ based on a dimerized G-quadruplex DNAzyme. *Analytical Chemistry*, *93*(18), 6907–6912.
34. Regelsberger, G., Jakopitsch, C., Rüker, F., Krois, D., Peschek, G. A. & Obinger, C. (2000). Effect of distal cavity mutations on the formation of compound I in catalase-peroxidases. *Journal of Biological Chemistry*, *275*(30), 22854–22861.
35. Rodríguez-López, J. N., Lowe, D. J., Hernández-Ruiz, J., Hiner, A. N. P., García-Cánovas, F. & Thorneley, R. N. F. (2001). Mechanism of reaction of hydrogen peroxide with horseradish peroxidase: identification of intermediates in the catalytic cycle. *Journal of the American Chemical Society*, *123*(48), 11838–11847.

Table 1. Sequences of oligonucleotides used in this study written in 5’ to 3’ direction

DNAzyme	Sequence
B730	ATTGGGAGGGATTGGGTGGG
B730-1	ATTGGGAGGGATTGGG**A**GGG**A**
B730-2	ATTGGGAGGGATTGGG**A**GGG**AAA**
B730-3	ATTGGGAGGGA**AA**GGGAGGG**A**
B730-4	ATTGGGAGGGATTGGGTGGG**AAAAA**
B730-5	ATTGGGAGGGA**AA**GGG**A**GGG**AAAAA**
B730-1.2	ATTGGGAGGGATTGGG**A**GGG**TC**
AS1411	GGTGGTGGTGGTTGTGGTGGTGGTGG
CatG4	TGGGTAGGGCGGGTTGGGAAA

Red and blue fonts indicate regions where modifications were carried out.

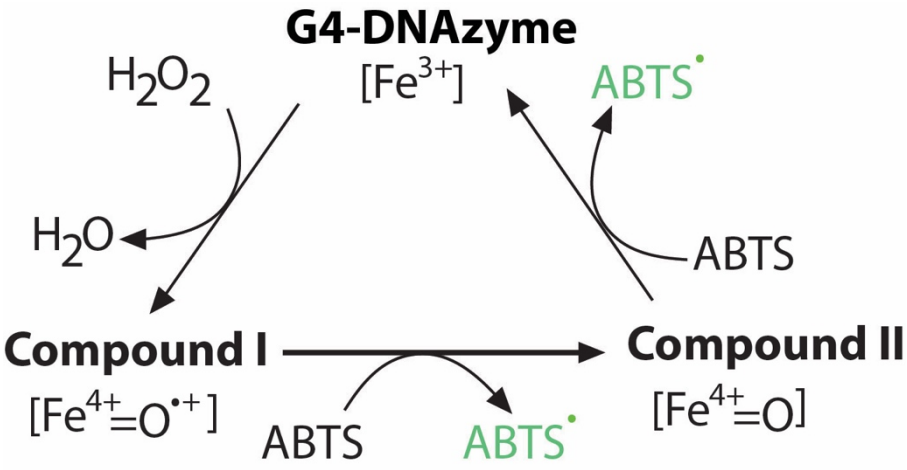

Figure 1: Peroxidase catalytic cycle. G4-DNAzyme complex reacts with and activates H_2O_2 to form the reactive Compound I (CI). CI oxidises a donor substrate (in this instance ABTS) using a mechanism similar to haem peroxidase-catalysed reactions and generating Compound II (CII) in the process. CII can react with H_2O_2 and initiate another round of ABTS oxidation. The reaction product (ABTS•) has a bright green colour with absorption maximum at 415 nm.

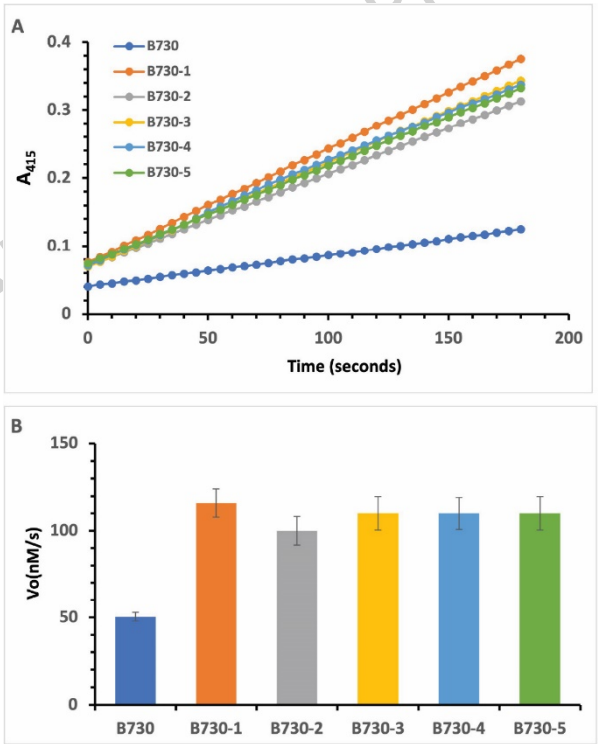

Figure 2: Catalytic activities of B730 and its redesigned variants. (A) Time-course profiles of ABTS oxidation monitored at 415 nm, showing real-time progression of peroxidase activity. (**B**) Initial velocities (V_0) of DNAzyme-catalyzed reactions, expressed in nM/s. Reaction conditions: 0.25 µM DNAzyme, 2.5 mM ABTS, 0.425 mM H_2O_2, 25 MES buffer pH 5.5, 20 mM KCl, 200 mM NaCl, 0.05% Triton X-100.

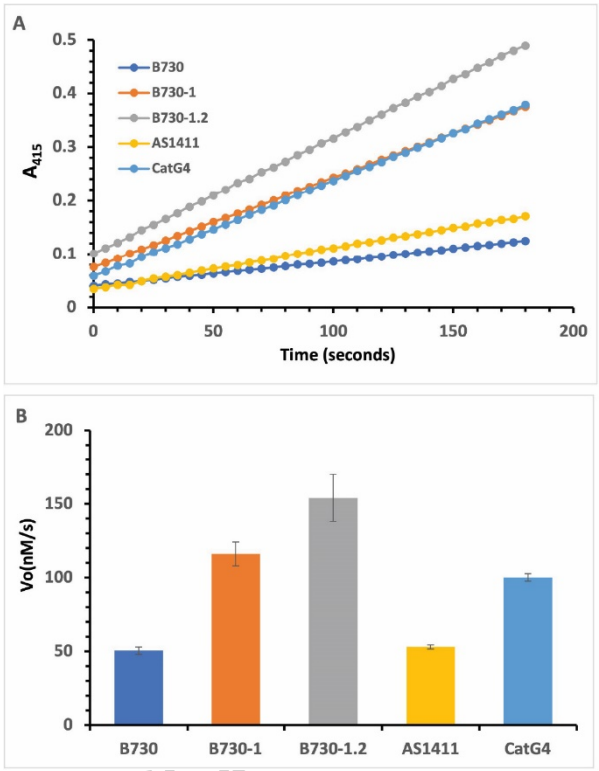

Figure 3: Comparative analysis of activities of B730 flanked with Adenine (A) nucleotide (B730-1) and Thymine-Cytosine (TC) dinucleotide (B730-1.2) with other high-activity DNAzyme (**A**) Time course reaction (**B**) Initial velocity (Vo expressed as nM/s). Reaction conditions and analysis are as described in Figure 2.

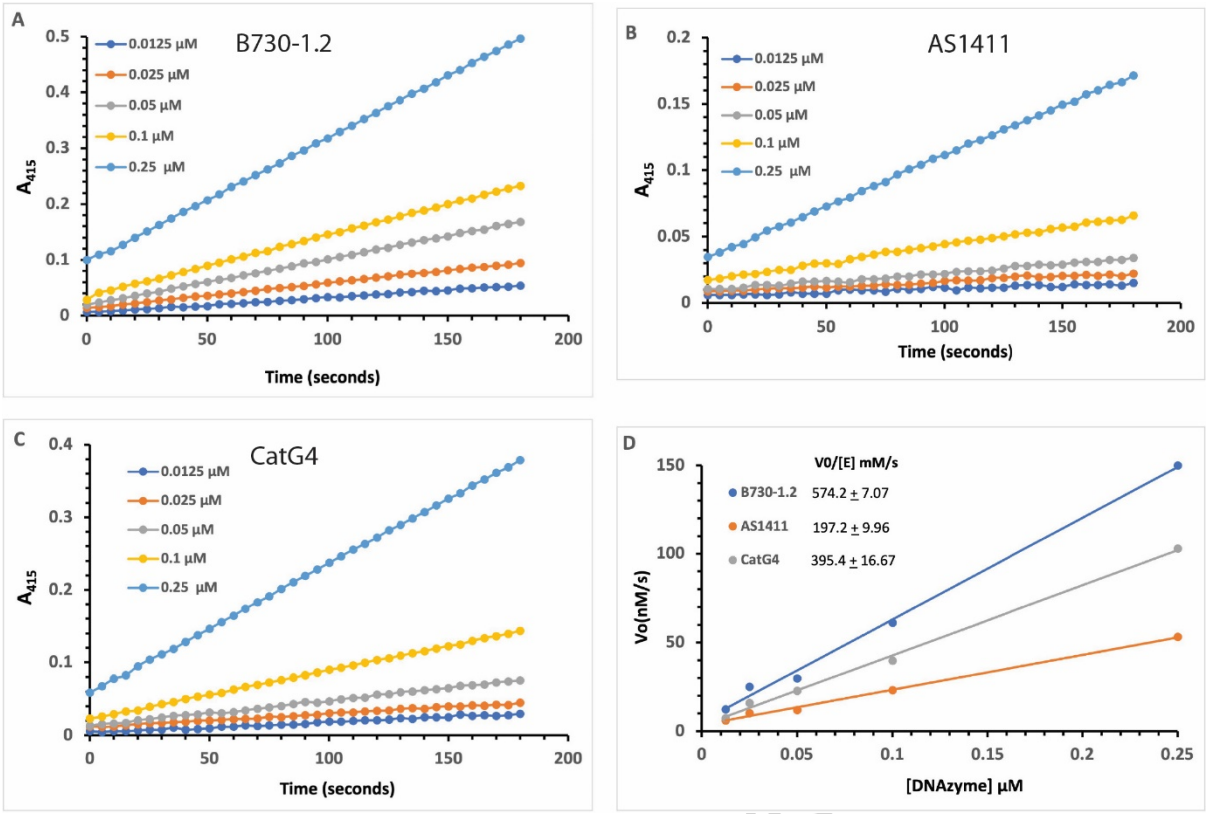

Figure 4. Effects of varying DNAzyme concentrations on oxidation of 2.5 mM ABTS at 0.425 H_2O_2 concentration. (**A**-**C**) Time courses of ABTS oxidation by B730-1.2, AS144 and CatG4 (**D**) Initial velocity of ABTS oxidation by B730-1.2, AS1411 and CatG4 at varying DNAzyme concentrations (0.0125-0.25 µM). Inset: Specific activity (V_0/[E]) of B730-1.2, AS1411 and CatG4.

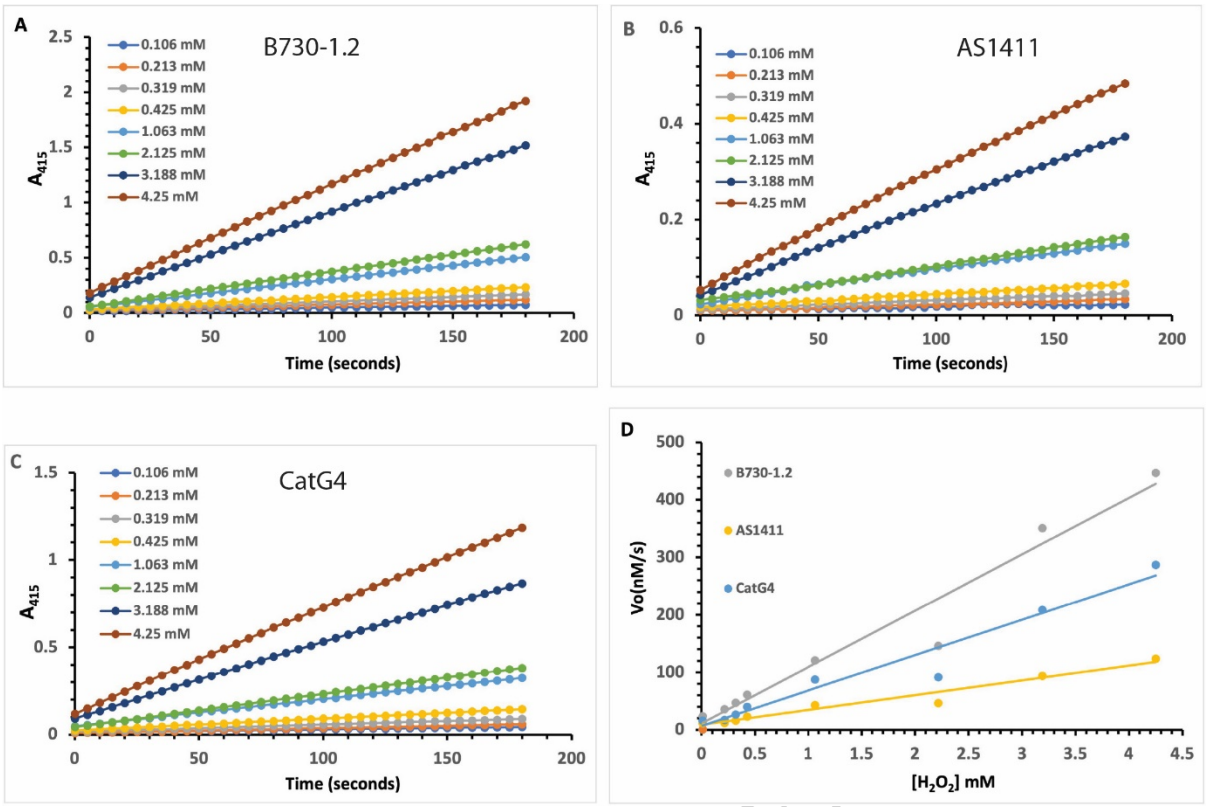

Figure 5. Effects of varying H_2O_2 concentrations on oxidation of 2.5 mM ABTS at low DNAzyme concentration (0.1 µM). (**A**-**C**) B730-1.2, AS144 and CatG4. (D) Initial velocity of ABTS oxidation by B730-1.2, AS1411 and CatG4 at varying H_2O_2 concentrations (0.106 - 4.250 mM).

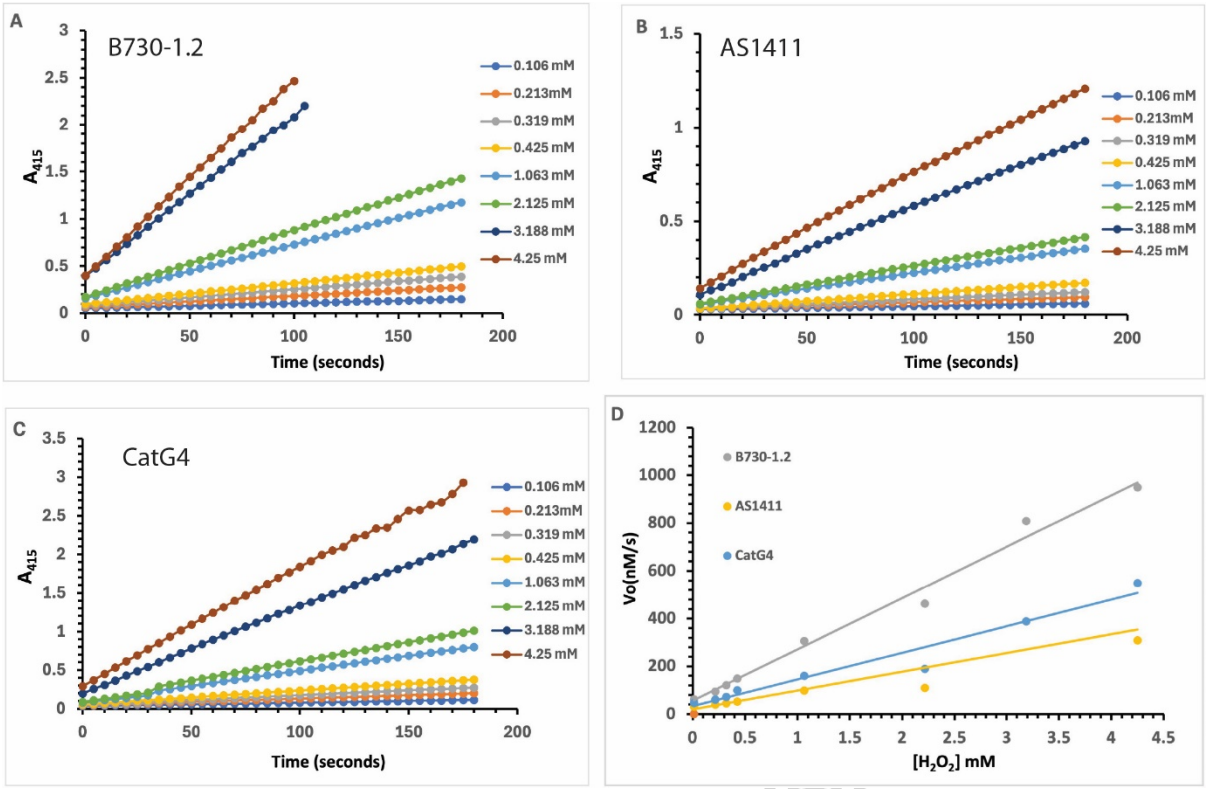

Figure 6. Effects of varying H_2O_2 concentrations on oxidation of 2.5 mM ABTS at moderate DNAzyme concentration (0.25 µM). (**A**-**C**) Time courses of ABTS oxidation by B730-1.2, AS144 and CatG4 at 0.106 - 4.250 mM H_2O_2 concentrations. (**D**) Initial velocity of ABTS oxidation by B730-1.2, AS144 and CatG4. H_2O_2 concentrations (0.106 - 4.250 mM).

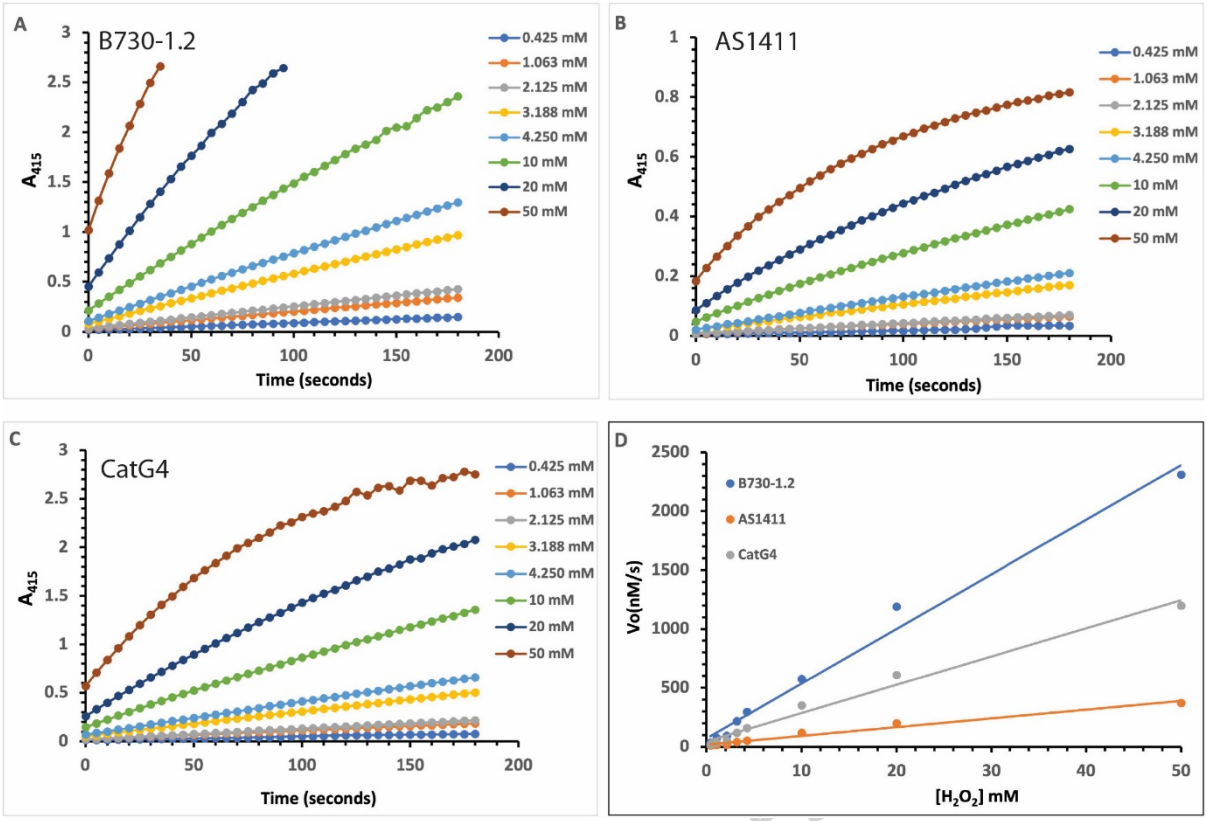

Figure 7. Effects of varying H_2O_2 concentrations on oxidation of 2.5 mM ABTS at very low DNAzyme concentration (0.05 µM). (**A-C**) Time courses of ABTS oxidation by B730-1.2, AS144 and CatG4 respectively at of 0.425 - 50 mM H_2O_2 concentrations. (**D**) Initial velocity of ABTS oxidation by B730-1.2, AS144 and CatG4. H_2O_2 concentrations (0.425 - 50 mM).

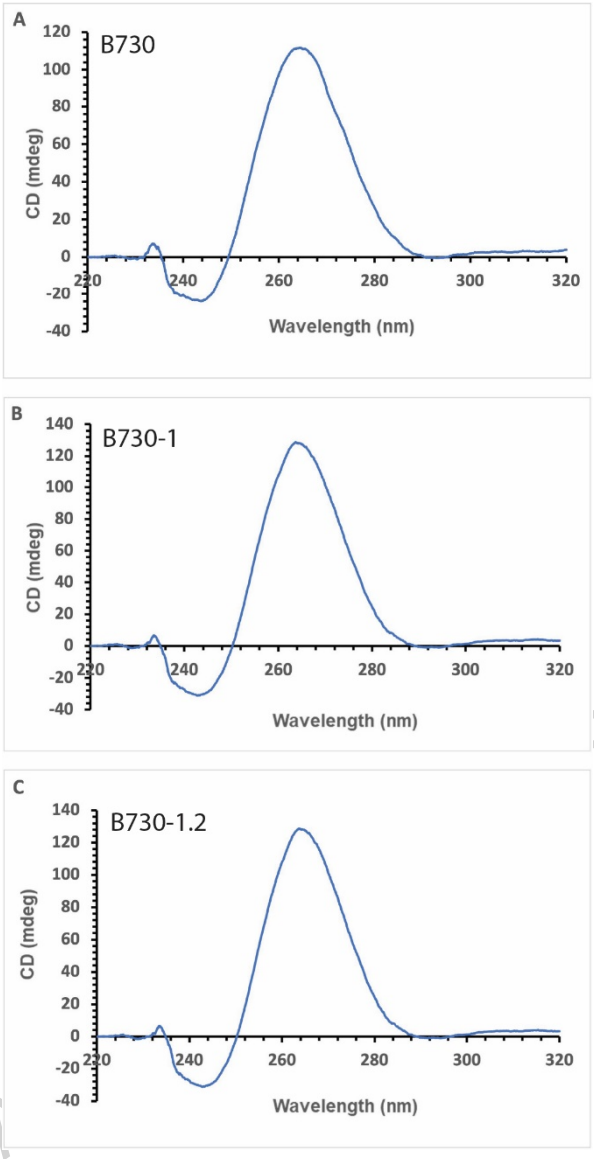

Figure 8. Circular dichroism spectral of B730, B730-1 and B730-1.2. (A) B730, (B) B730-1, and (C) B730-1.2. Spectra (320–220 nm) were recorded for 10 μM G4 oligonucleotides in 25 mM MES buffer (pH 5.5) containing K^+.

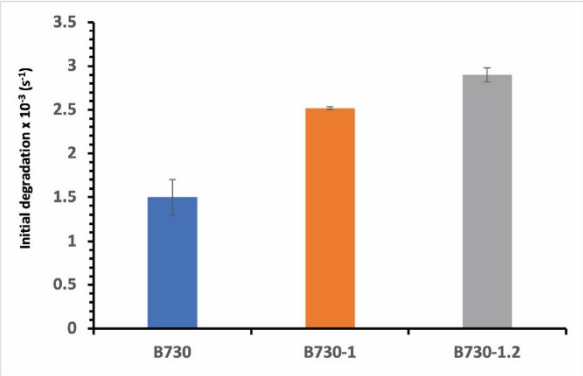

Figure 9. Relative compound I formation by B700, B730-1 and B730-1.2 based on hemin degradation monitored at 404 nm after adding 0.425 mM H_2O_2 and 1 μM G4 DNAzyme in MES buffer pH 5.5 (B730-1.2 indicates faster rate of compound I formation than other DNAzyme).

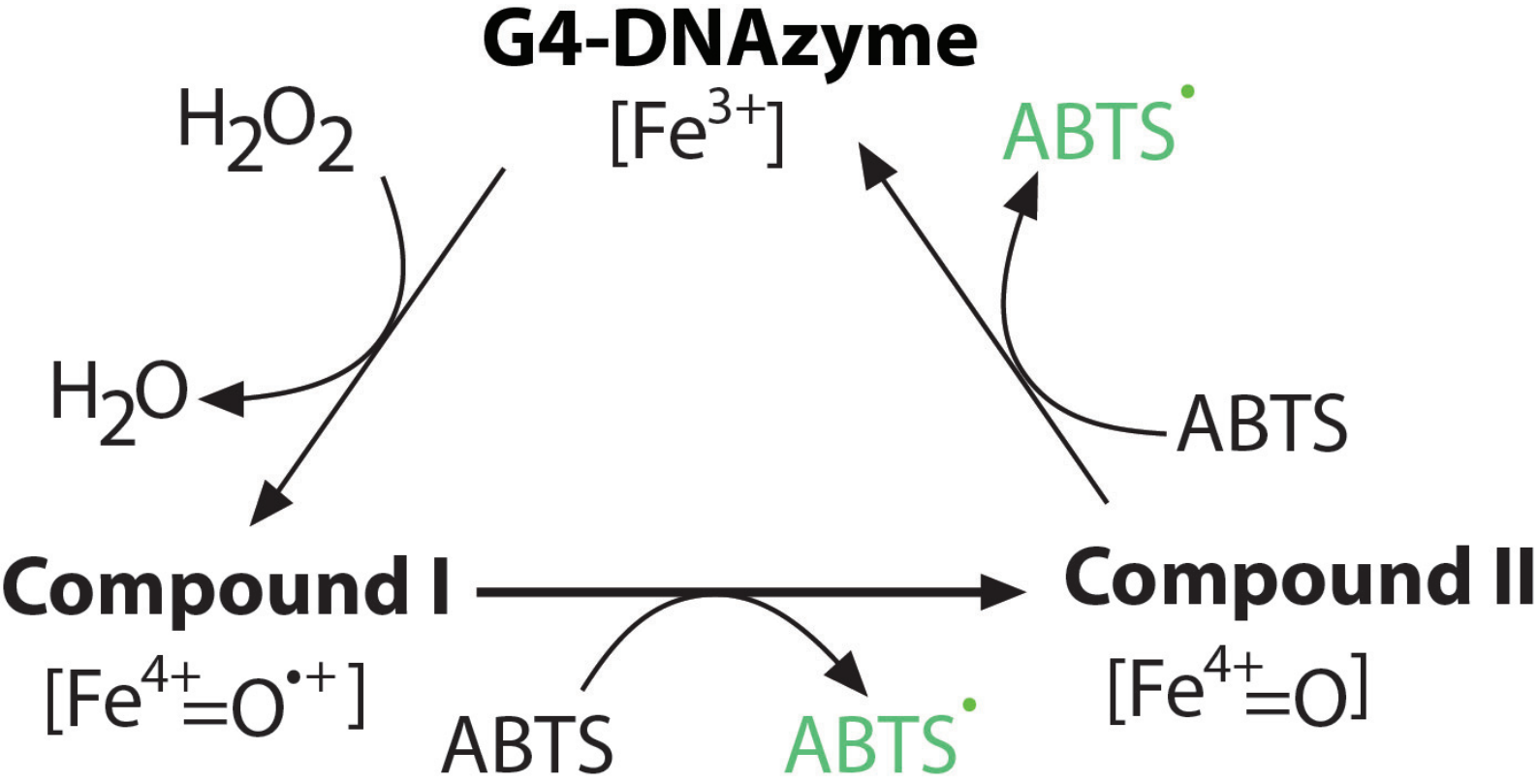
G4-DNAzyme
[Fe3+]
H2O2
H2O
ABTS•
ABTS
Compound I
[Fe4+=O•+]
Compound II
[Fe4+=O]
ABTS
ABTS•

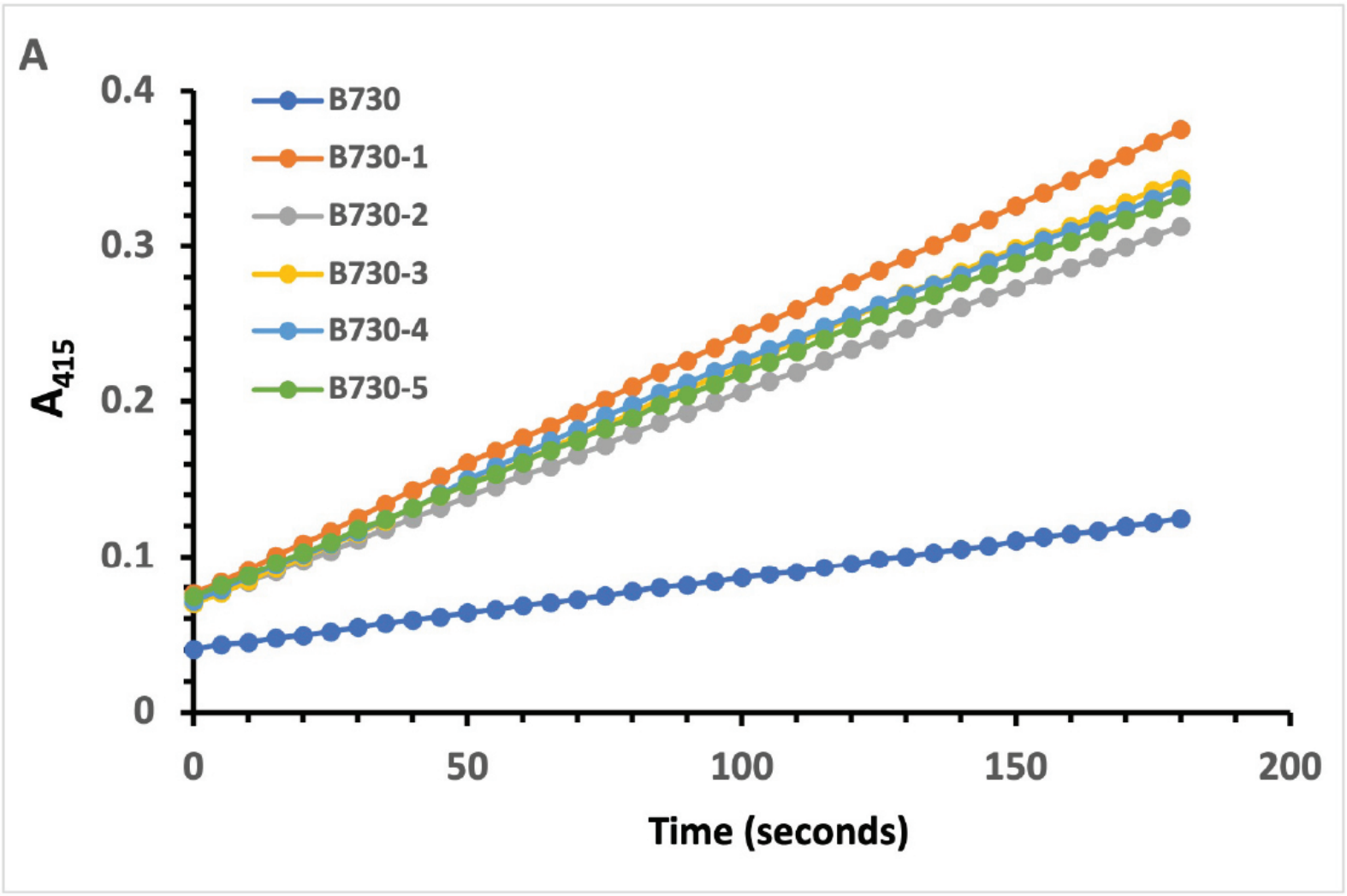
A
0.4
0.3
0.2
0.1
0
A_{415}
B730
B730-1
B730-2
B730-3
B730-4
B730-5
0
50
100
150
200
Time (seconds)

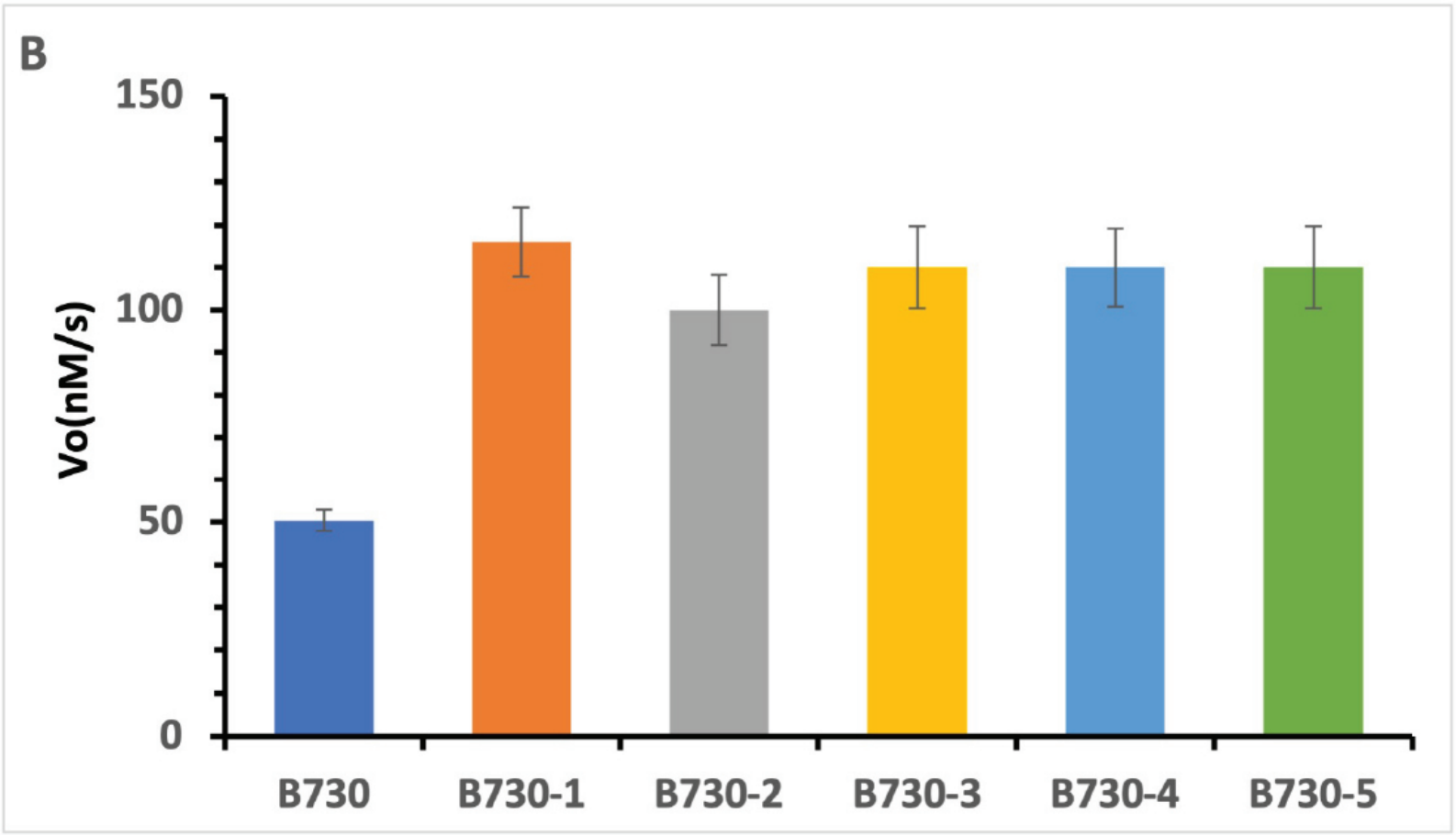
B
150
100
50
0
Vo(nM/s)
B730
B730-1
B730-2
B730-3
B730-4
B730-5

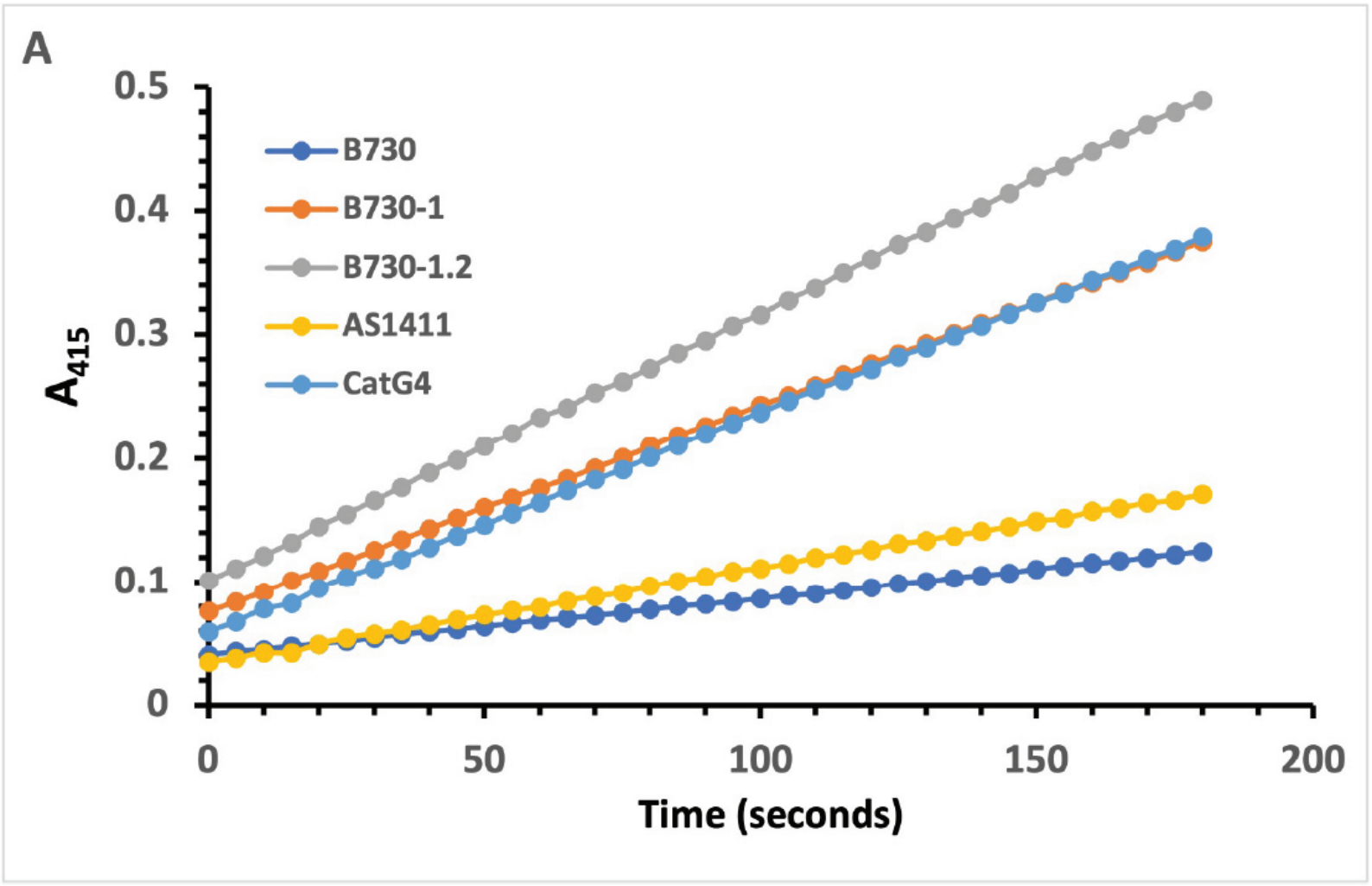
A
0.5
0.4
0.3
0.2
0.1
0
A_{415}
B730
B730-1
B730-1.2
AS1411
CatG4
0
50
100
150
200
Time (seconds)

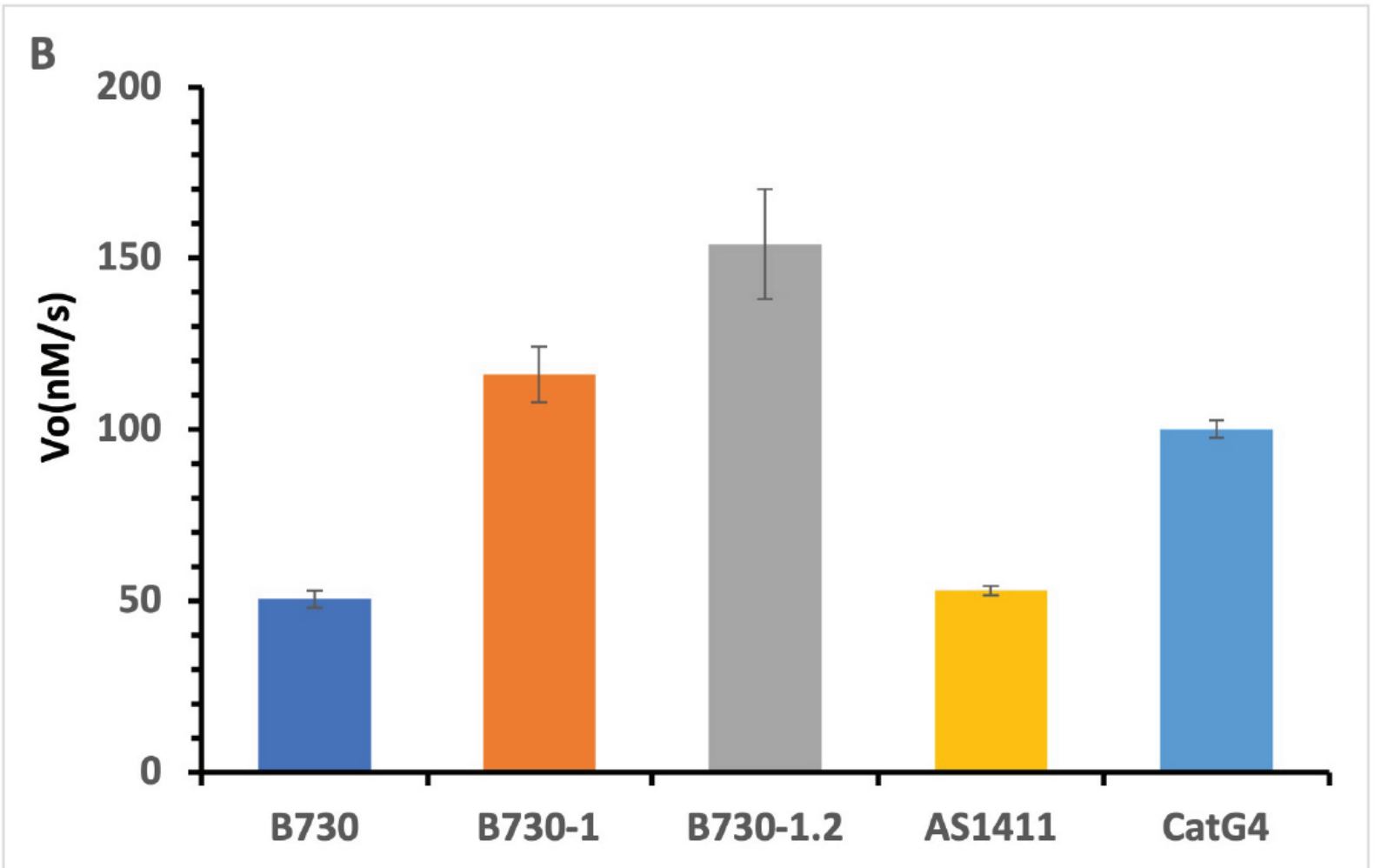
B
200
150
100
50
0
Vo(nM/s)
B730
B730-1
B730-1.2
AS1411
CatG4

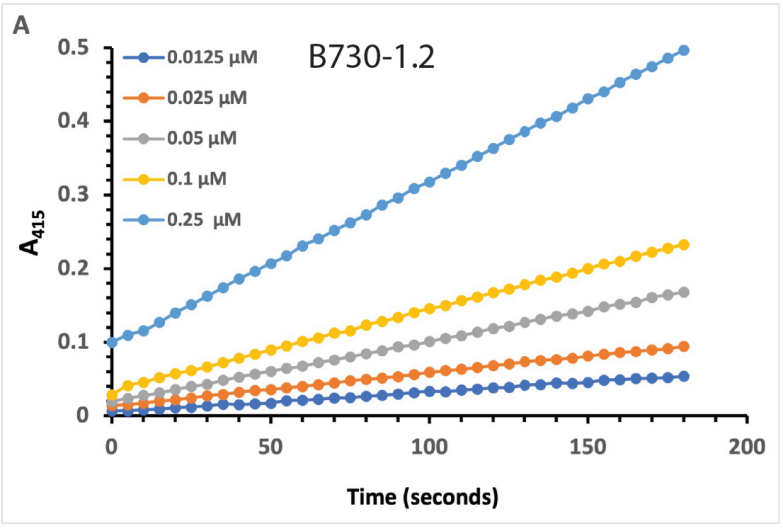
A
B730-1.2
0.0125 µM
0.025 µM
0.05 µM
0.1 µM
0.25 µM
A415
Time (seconds)

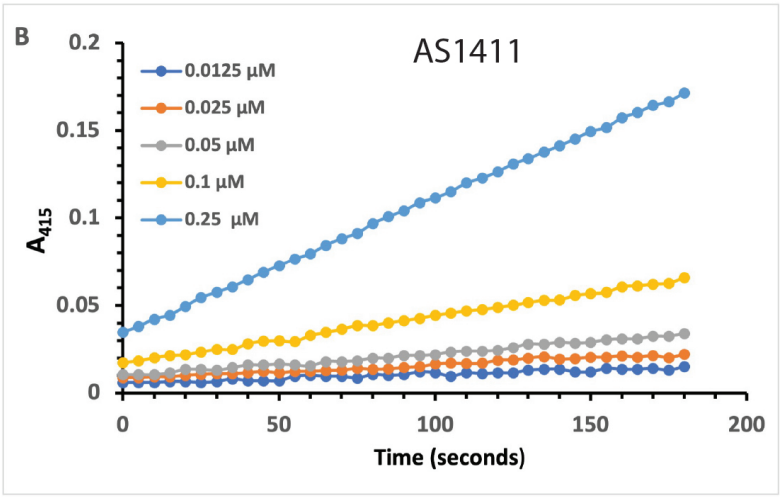
B
AS1411
0.0125 µM
0.025 µM
0.05 µM
0.1 µM
0.25 µM
A415
Time (seconds)

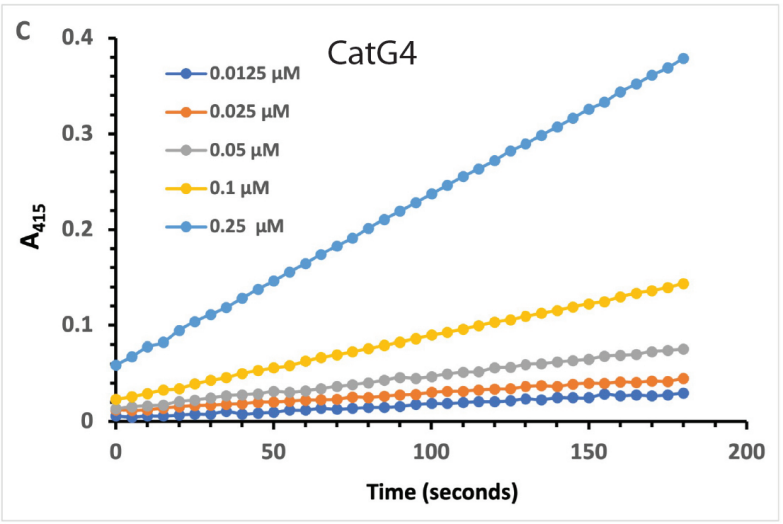
C
CatG4
0.0125 µM
0.025 µM
0.05 µM
0.1 µM
0.25 µM
A415
Time (seconds)

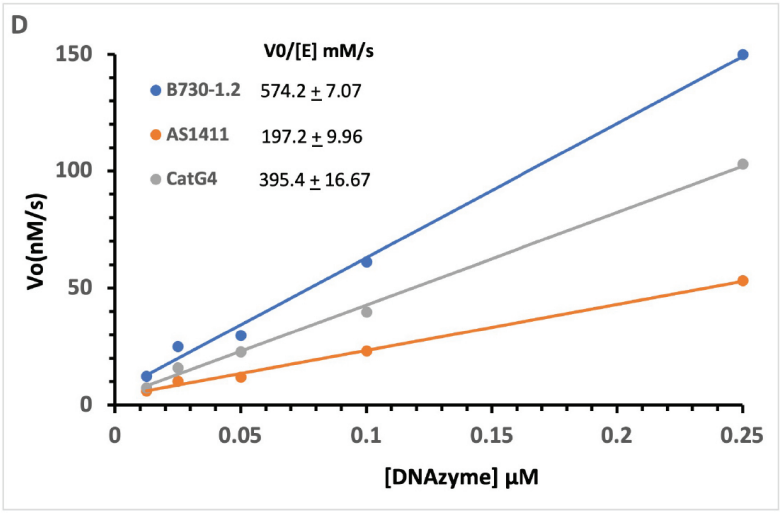
D
V0/[E] mM/s
B730-1.2 574.2 ± 7.07
AS1411 197.2 ± 9.96
CatG4 395.4 ± 16.67
Vo(nM/s)
[DNAzyme] µM

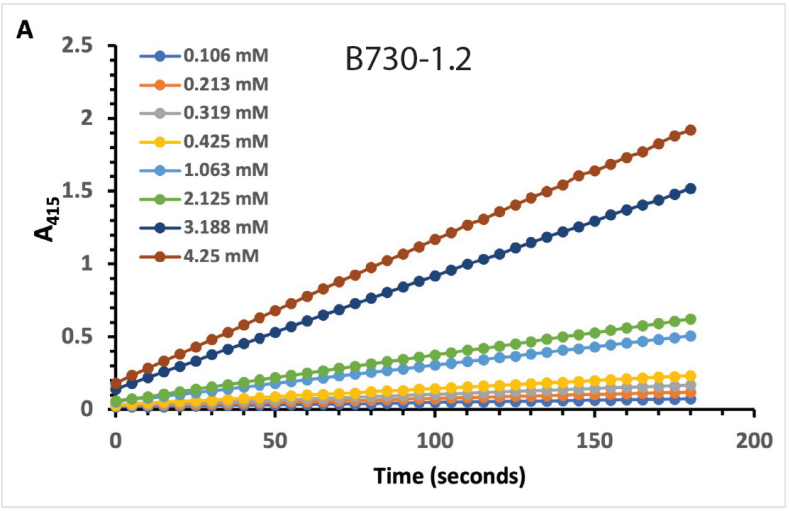
A
B730-1.2
0.106 mM
0.213 mM
0.319 mM
0.425 mM
1.063 mM
2.125 mM
3.188 mM
4.25 mM
A415
Time (seconds)

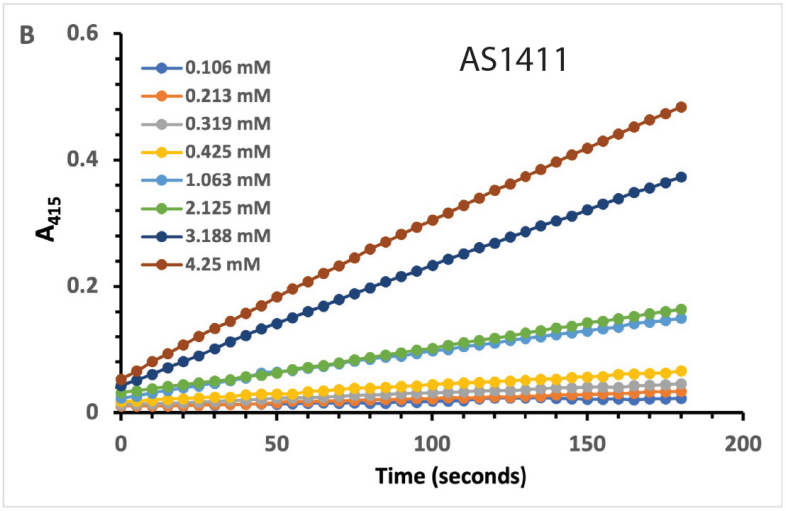
B
AS1411
0.106 mM
0.213 mM
0.319 mM
0.425 mM
1.063 mM
2.125 mM
3.188 mM
4.25 mM
A415
Time (seconds)

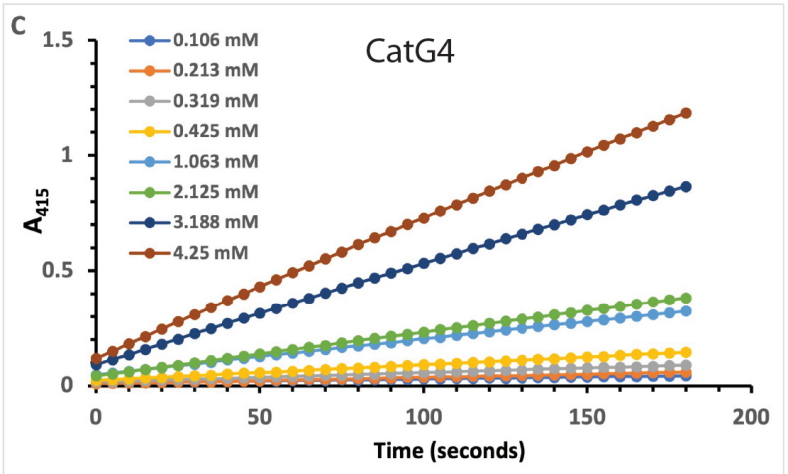
C
CatG4
0.106 mM
0.213 mM
0.319 mM
0.425 mM
1.063 mM
2.125 mM
3.188 mM
4.25 mM
A415
Time (seconds)

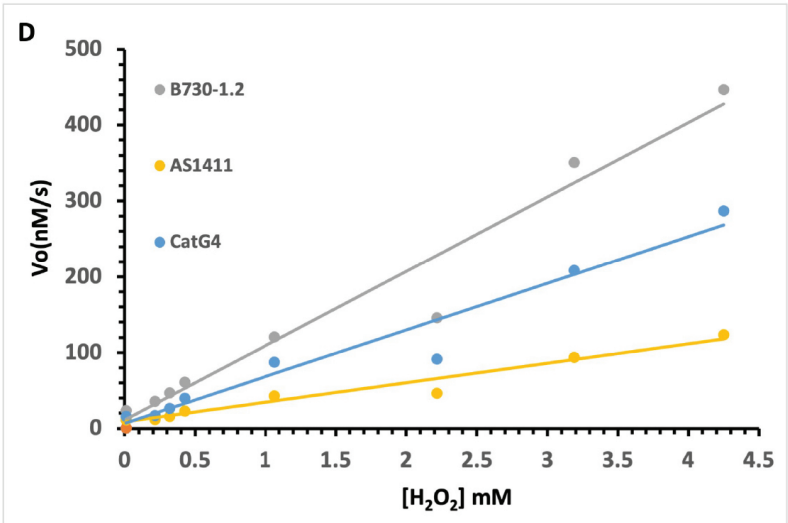
D
B730-1.2
AS1411
CatG4
Vo(nM/s)
[H2O2] mM

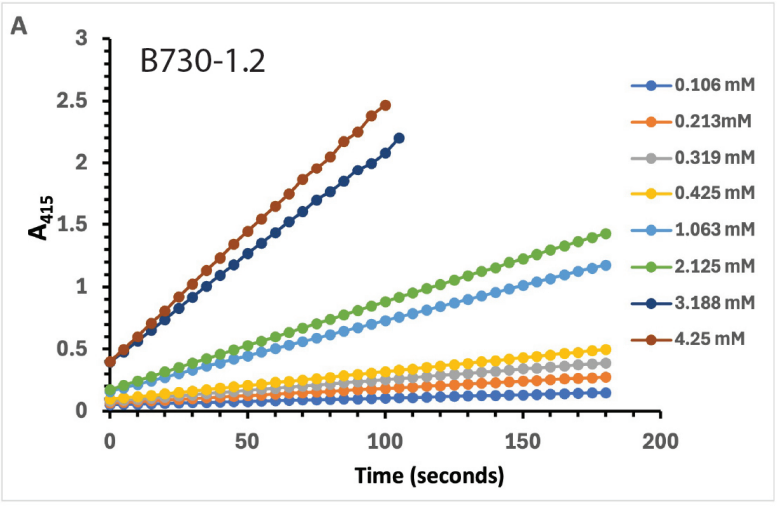
A
B730-1.2
A_{415}
Time (seconds)
0.106 mM
0.213mM
0.319 mM
0.425 mM
1.063 mM
2.125 mM
3.188 mM
4.25 mM

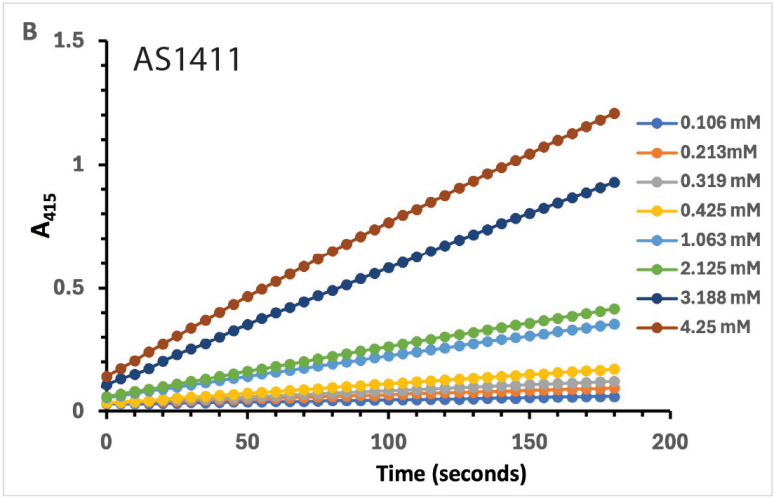
B
AS1411
A_{415}
Time (seconds)
0.106 mM
0.213mM
0.319 mM
0.425 mM
1.063 mM
2.125 mM
3.188 mM
4.25 mM

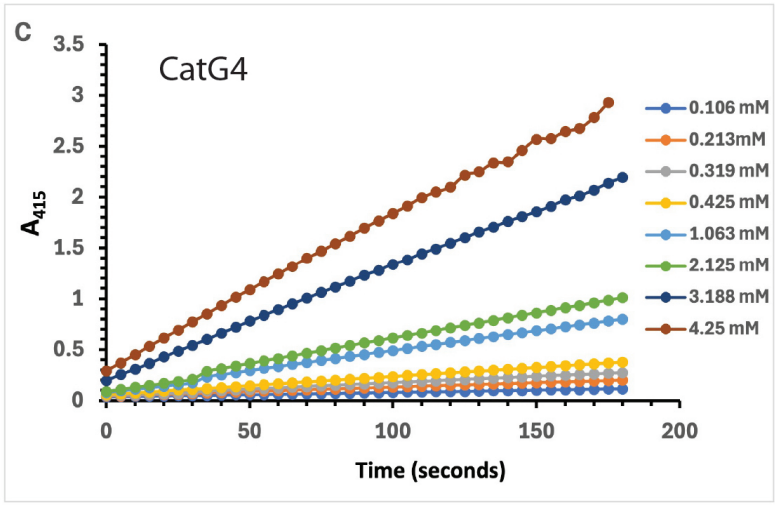
C
CatG4
A_{415}
Time (seconds)
0.106 mM
0.213mM
0.319 mM
0.425 mM
1.063 mM
2.125 mM
3.188 mM
4.25 mM

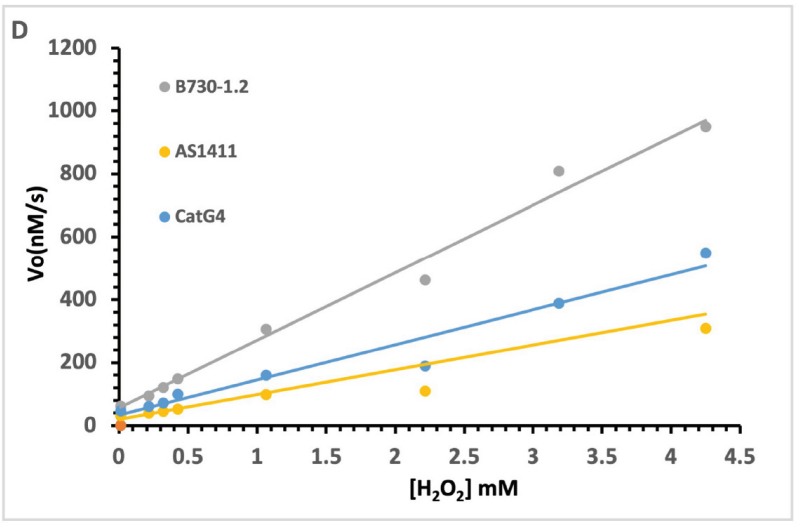
D
Vo(nM/s)
$[H_2O_2]$ mM
B730-1.2
AS1411
CatG4

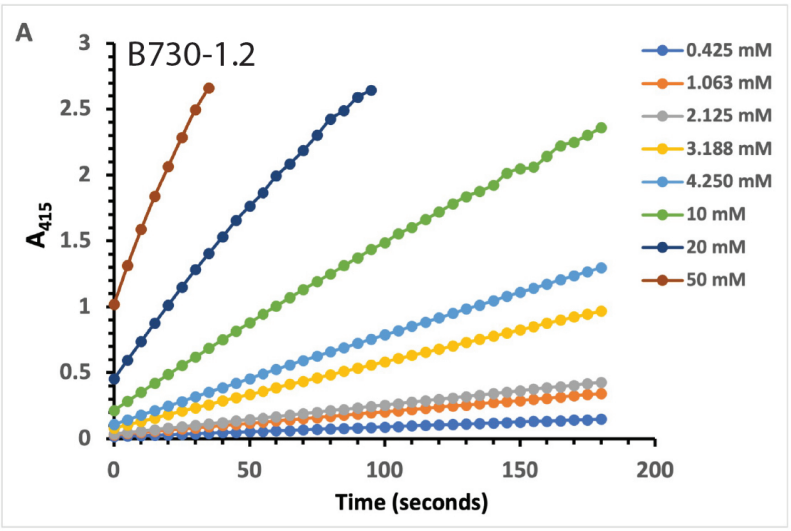
A
B730-1.2
A_{415}
Time (seconds)
0.425 mM
1.063 mM
2.125 mM
3.188 mM
4.250 mM
10 mM
20 mM
50 mM

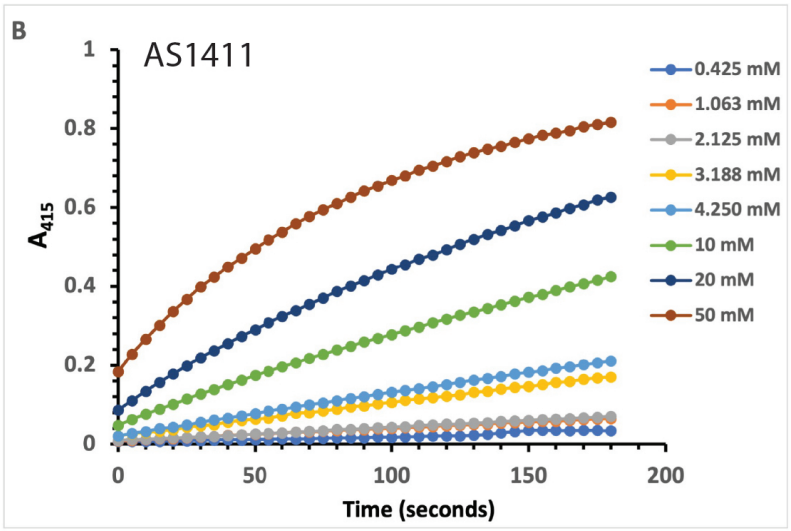
B
AS1411
A_{415}
Time (seconds)
0.425 mM
1.063 mM
2.125 mM
3.188 mM
4.250 mM
10 mM
20 mM
50 mM

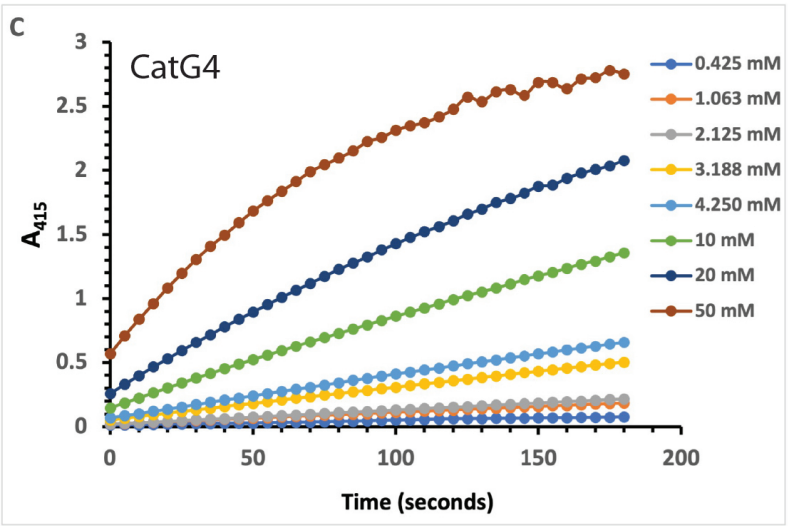
C
CatG4
A_{415}
Time (seconds)
0.425 mM
1.063 mM
2.125 mM
3.188 mM
4.250 mM
10 mM
20 mM
50 mM

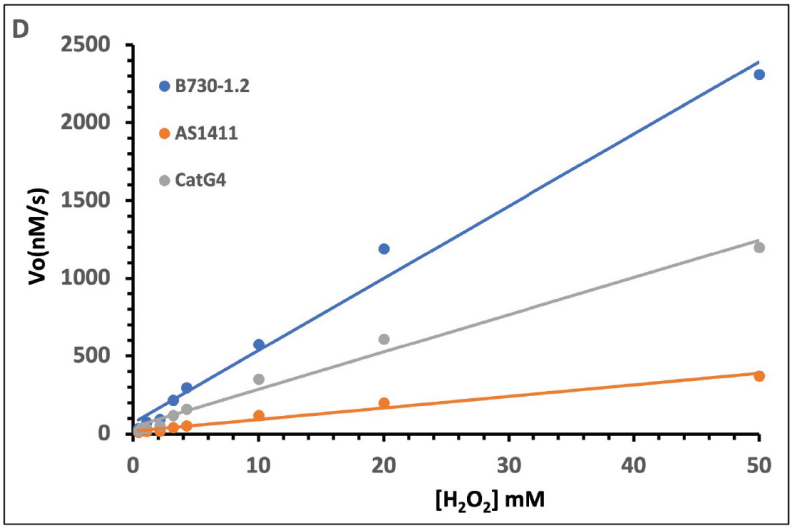
D
Vo(nM/s)
$[H_2O_2]$ mM
B730-1.2
AS1411
CatG4

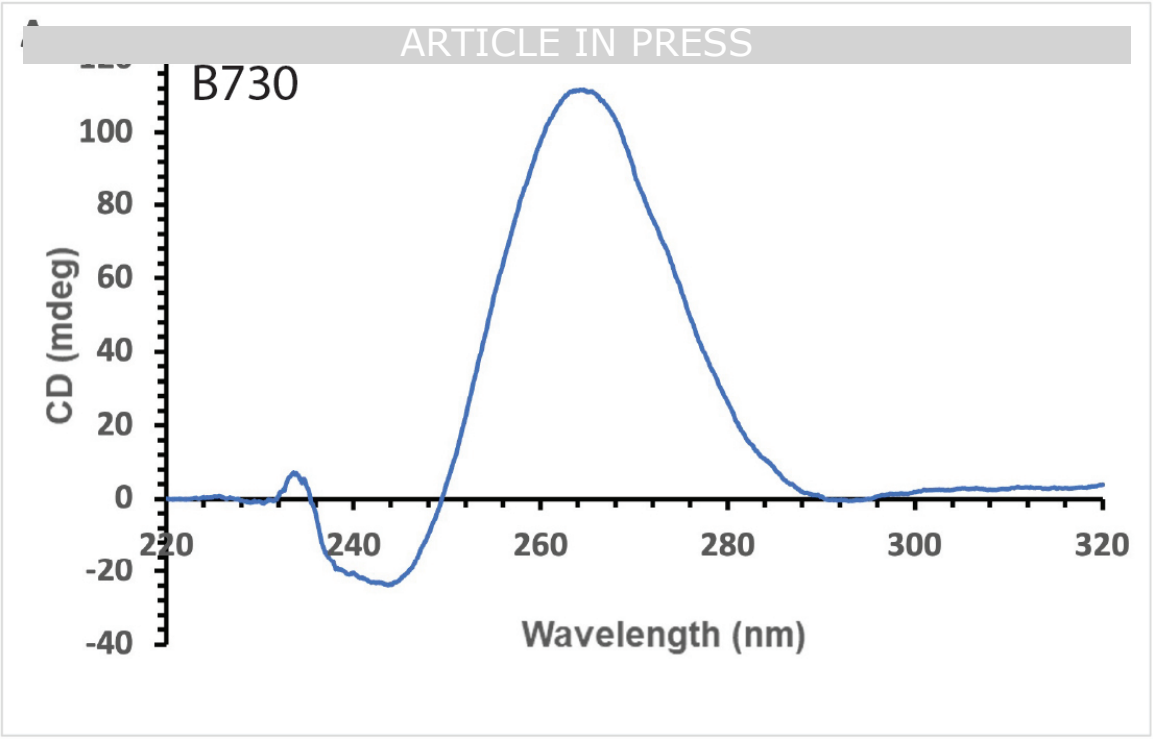

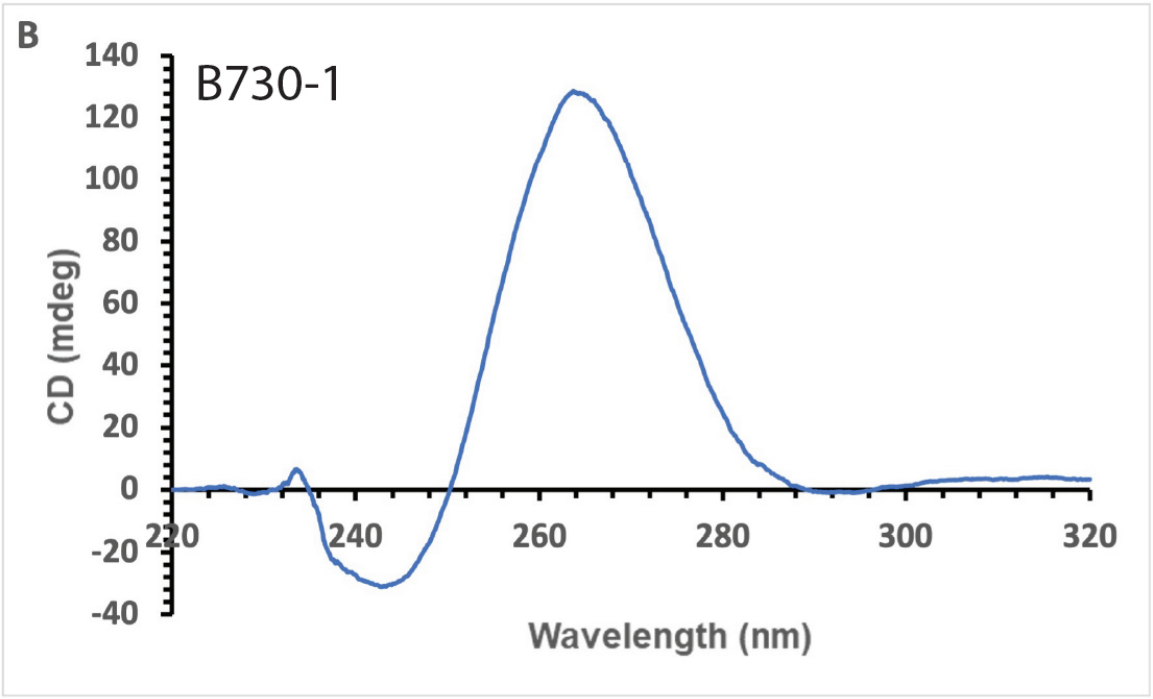

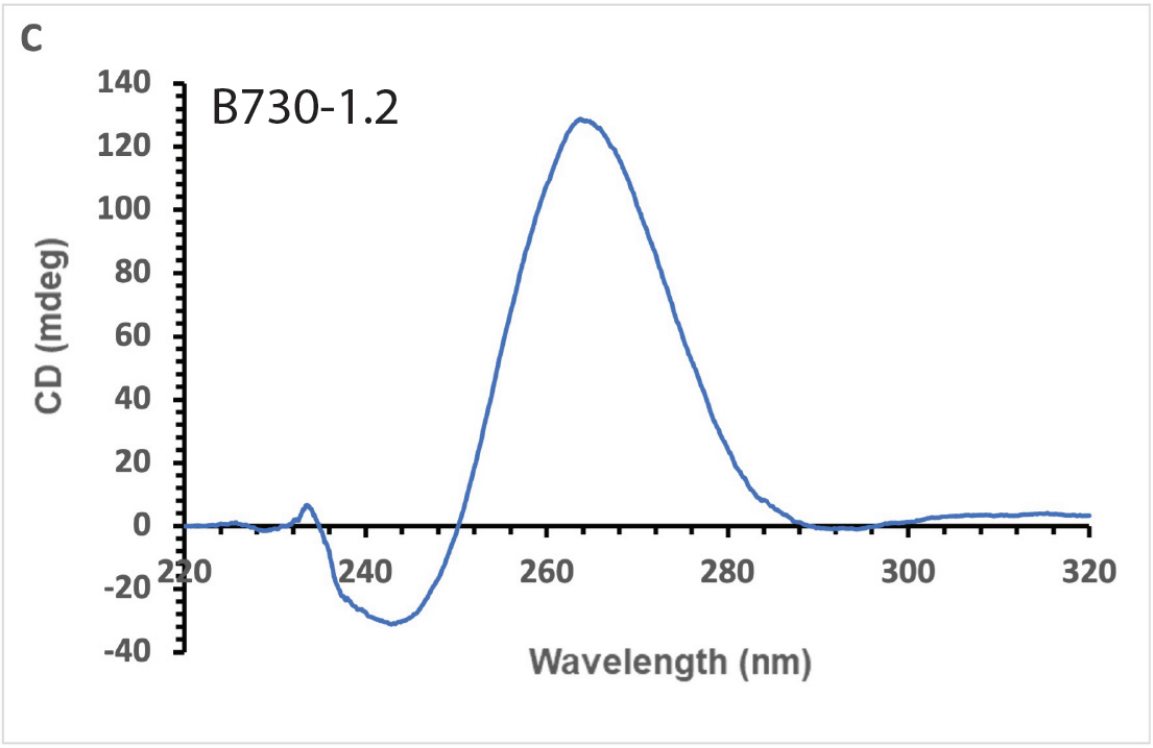

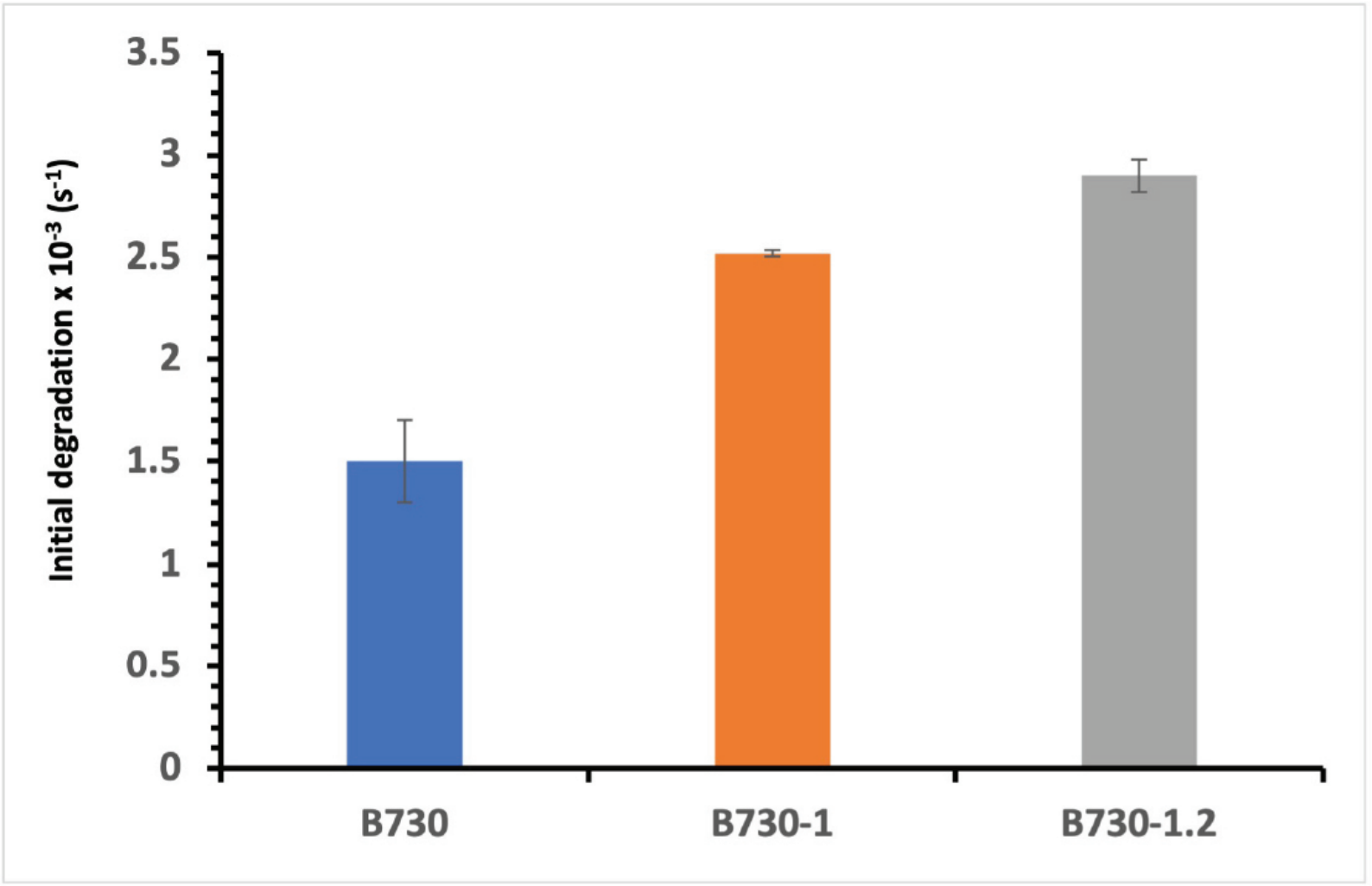
Initial degradation x 10-3 (s-1)
3.5
3
2.5
2
1.5
1
0.5
0
B730
B730-1
B730-1.2

DNAzyme	Sequence
B730	ATTGGGAGGGATTGGGTGGG
B730-1	ATTGGGAGGGATTGGGAGGGA
B730-2	ATTGGGAGGGATTGGGAGGGAAA
B730-3	ATTGGGAGGGAAAGGGAGGGA
B730-4	ATTGGGAGGGATTGGGTGGGAAAAA
B730-5	ATTGGGAGGGAAAGGGAGGGAAAAA
B730-1.2	ATTGGGAGGGATTGGGAGGGTC
AS1411	GGTGGTGGTGGTTGTGGTGGTGGTGG
CatG4	TGGGTAGGGCGGGTTGGGAAA